



Hydrological Modeling and Evaluation of Water Balance Over the Complex Topography of Nile Basin Headwaters: The Case of Ghba River, Northern Ethiopia

Mehari Gebreyohannes Hiben ^{a, b, *}, Admasu Gebeyehu Awoke ^a, Abraha Adugna Ashenafi ^c

^a School of Civil and Environmental Engineering, Addis Ababa University, Addis Ababa Institute of Technology (AAiT), Addis Ababa, Ethiopia

^b MG Water Resources consultancy Firm, Mekelle, Tigray, Ethiopia

^c The Ministry of Water and Energy (MWE), Addis Ababa, Ethiopia

*Corresponding Author Email: hiben123@gmail.com

DOI: <https://doi.org/10.54392/irjmt2363>

Received: 26-07-2023; Revised: 22-10-2023; Accepted: 28-10-2023; Published: 03-11-2023



Abstract: Water resource evaluation, management, and conservation at the local, national, and international levels depend on an accurate understanding of the hydrological processes. In data-poor environments and topographically complicated areas like the Ghba subbasin in the headwaters of the Nile River, the function of hydrological models is crucial. The primary goal of this study is to use the WEAP model to simulate the hydrology of the Ghba basin. This is because recent hydrological behaviour has changed significantly and resulted in a serious water deficit. The minimal satisfactory performance limit for the monthly stream flow variable was strongly attained by the multi-variable calibration scenario ($R^2 = 0.82$, $NSE = 0.82$, $IA = 0.80$, $RSR = 0.87$ and $PBIAS = 9\%$ for calibration scenario; and $R^2 = 0.78$, $NSE = 0.81$, $IA = 0.70$, $RSR = 0.80$ and $PBIAS = 11.5\%$ for validation scenario). Evapotranspiration makes up 63.4% of the water balance, according to the model simulation, while surface runoff, interflow, baseflow and groundwater recharge accounting for 11.1%, 11.8%, 5.4% and 8.3%, respectively. The simulated average annual streamflow at the subbasin outlet is 16.33 m³/s. The simulated monthly minimum flow occurs in January with an average flow of 1.78 m³/s and a coefficient of dispersion of 0.45. Maximum flows occur in July and August, with an average flow of 53.57 m³/s and a coefficient of dispersion of 0.19. The main rainy season was shown to have a larger spatial distribution of simulated runoff, and the average annual recharge value is 53.5 mm. The study's conclusions indicated that both surface water harvesting and groundwater extraction might be used for reliable water distribution to the subbasin's continuously increasing sectoral water demand.

Keywords: WEAP Model, Hydrology, Ghba subbasin, Groundwater

1. Introduction

The Ghba subbasin receives a mean annual precipitation of 641mm [1, 2]. The subbasin is facing growing anthropogenic and socioeconomic activities leading to severe water shortages in recent years [3, 4]. In spatiotemporal dimensions of hydrological processes understanding the hydrological characteristics is vital to evaluate alterations in a hydrologic system's dynamic responsiveness [5]. Change of existing land management practices in a catchment affects the hydrological cycle that comprises precipitation, evapotranspiration (ET), runoff, flow of groundwater, recharge, and infiltration and their connections in the atmosphere, land surface, and subsurface that drives movement, distribution, and transformation of water from one configuration to another [6-9]. Many researches verified that Land Use / Land Cover (LULC) changes dramatically govern the timing and magnitude of

extreme events [10, 11, 12]. Thus, such kind of complex relationship between hydrological processes and human-induced environmental changes has been always issuing questions to scientific community to understand the complex nature of the system. Therefore, for hydrologic parameter estimation, models are commonly used. In general models are the simplification of reality [13, 14], and therefore, the results are not always accurate. However, they can be useful when they are interpreted using professional expertise. I want to emphasize the contention by Abbott that "A model is a collection of signs that serve as a sign" [15] as stated by Price [16]. Accordingly, to simulate the hydrological processes, hydrological models are utilized. so as to improve our knowledge of understanding to the system and prediction of hydrologic processes [17-19]. In the recent studies, the usage of hydrologic models is common. to properly characterize the catchments

properties using target parameter prediction depending on data input [20, 21]. Furthermore, models that have good measured and simulated data agreement can be applied to a variety of purposes, including assessing the effects of changing input factors like climate change, land-use/land cover (LULC) change, intervention of structures in the river system, and so on which will give a chance to set scenarios and analysis for different adaptation options [22, 23-25]. Different regions have used hydrological models, ranging from conceptual to fully physically based distributed models. These types of models have their own merits and demerits [26-28]. fully distributed physical models are suitable to precisely define the method of the hydrology in a complex catchment [29, 30] However, the model complexity Vs over parameterization of models makes model calibration extremely tough [31]. The over-parameterization tricky is not the main worry of conceptual models, but they frequently fail to give the non-linear dynamics of catchment characteristic which is important in studying the hydrological response to the dynamics of environmental changes [32, 33].

To simulate any potential interactions between various elements, physical-based models can be employed in to generate time series hydrologic features [34, 35]. These sets of modeling systems, for instance, MIKE HYDRO Basin [36], SWAT [37] and the WEAP [38] are a few modelling system examples that have been widely used throughout the world. At this time, Consecutive streamflow declines have been a problem for the Ghba subbasin [39], and different researches by Gebremicael, Mohamed [40], Gebremicael, Mohamed [32], Mekelle [41], and Zenebe, Vanmaercke [42] has testified the reduction of streamflow due to human-induced environmental changes, for example, land development thereafter, it becomes difficult to satisfy the economic scarcity of water resulting from the increasing demand for water supplies (domestic and nondomestic), irrigation, and the water requirement for environmental flow in the Ghba subbasin [4, 43, 44]. Additionally, the possible effects of climate change have made it more difficult to sustain water resources [40]. a thorough awareness of the amount and quality of the water resources that are available leads to the efficient water resource management and allocation strategies in the subbasin [45-47]. Thus, a model-based surface water resource potential assessment can be done by modeling the hydrologic processes that occur naturally, climate change, human-induced effects, and water resource management strategies [48-50]. Currently, management and distribution of water resources policies are primarily used water resource scenario analysis using models to look for different alternative options [51, 52]. To be able to manage and allocate water resources effectively, modeling of such resources is a must and a key component of scenario analysis [53]. Therefore, different modelling system platforms can be applied Depending on the particular objective the scenario analysis. The

development of several hydrological studies utilizing physically based models has occurred all across the world [54-56] The hydrological models, in particular in the Ghba subbasin, have been created by Aredehey, Mezgebu [44], Gebremicael, Mohamed [32], Ashenafi [57] and Bizuneh [58] to evaluate the hydrologic response of the subbasin. They have studied the Ghba subbasin's hydrologic process, including Surface runoff, ETo, interflow, and baseflow. The Wflow PCRaster/Python framework and SWAT models were utilized in similar investigations. By Gebremicael, Mohamed [32], Aredehey, Mezgebu [44] to evaluate the effects of environmental changes brought on by humans in the Ghba subbasin. However, The Ghba subbasin has not yet been subjected to water resource models for management and distribution methods for water along with hydrological models.

Taking this into consideration, The WEAP modeling system was developed by the Stockholm Environmental Institute. [38], and has been chosen to be applied in the Ghba subbasin to build the hydrological model for improved water allocation. The WEAP software is a very advanced system for modeling water resources that comprises choices to model both the management of and the usual rainfall-runoff processes executed water system [59, 60]. Many studies have been successfully used the WEAP modeling system across many regions of the world [61, 62-64] to model urban and agricultural catchments used in the simulation of land use planning considering climate impact, and population growth. In the current study the soil moisture method from the five hydrological options/methods of the model structure installed in the WEAP software is selected. The effectiveness of employing the WEAP model, as needed for developing the Ghba subbasin hydrological model was assessed. The model evaluation was done using model indices evaluation criteria for the simulation period of the hydrological processes. Hence, the 1st section contains the general introduction and literature review, and the rest of the paper is organized as follows: Section 2 contains the methodology [65]. Section 3 contains the results. The study's conclusions and suggestions are included in Section 4.

2. Data and Methods

2.1 Study Area

The Ghba subbasin is located in northern Ethiopia and covers from 38°38' to 39°48' Eastern longitudes and 13°14' to 14°16' northern latitudes as can be seen Figure 1. Mekelle, the capital of the Tigray regional state, is located inside the Ghba subbasin, which has a total size of around 5125 km². It creates Tekeze River basin's Upper headwaters, one of the principal Nile River tributaries [32]. North and north-eastern highlands and hills, as well as highlands in the catchment's centre, define the topography [66]. The major Tekeze River is formed at Chemey by the

confluence of several rivers that split the central highlands. These rivers flow towards the subbasin's southwest corner [67]. Figure 1 shows that between the subbasin outlet and the highest point of the Mugulat Mountains, which are adjacent to the town of Adigrat, the

elevation above sea level ranges from 930 to 3,300 meters [68]. The catchment's mean elevation is 2144 meters, and its standard deviation is 361 meters, proving that topography is highly rough [69].

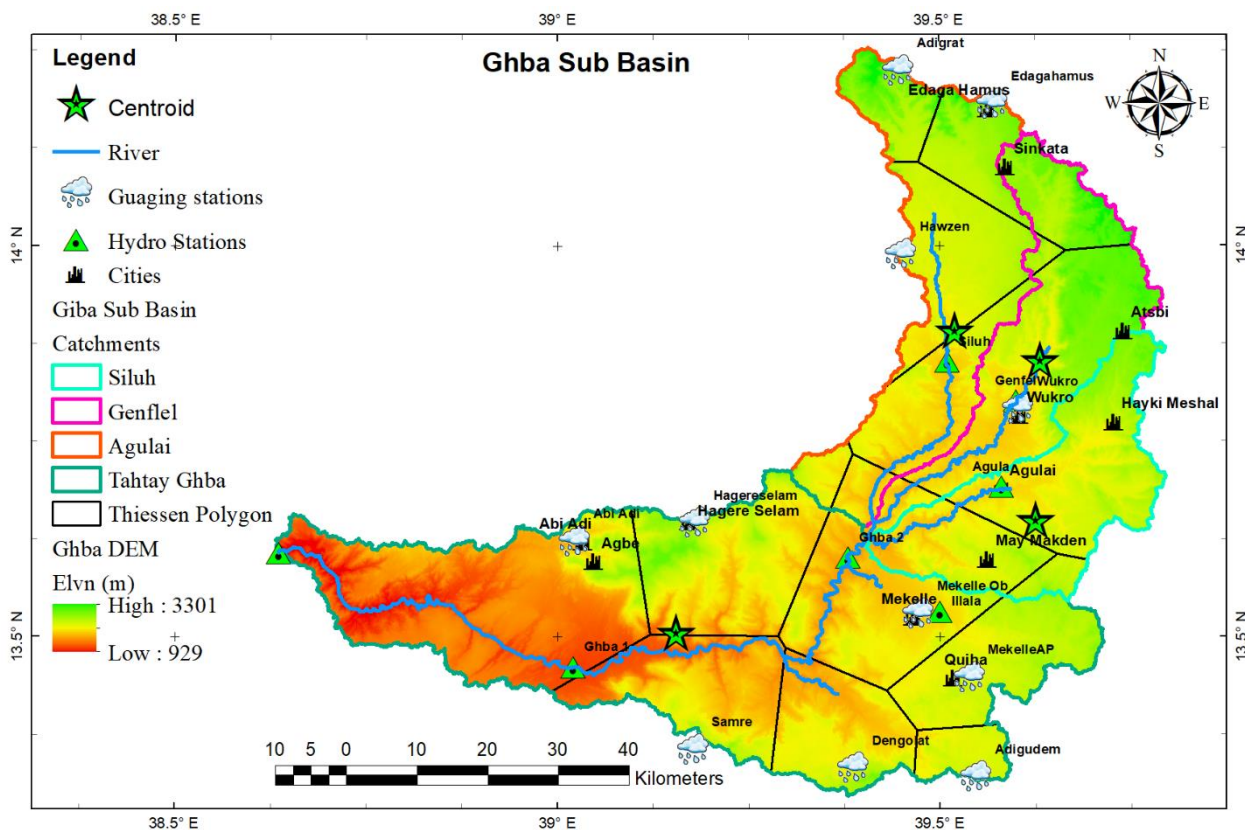


Figure 1. Thiessen polygon weighted precipitation and WEAP time series expression for each catchment

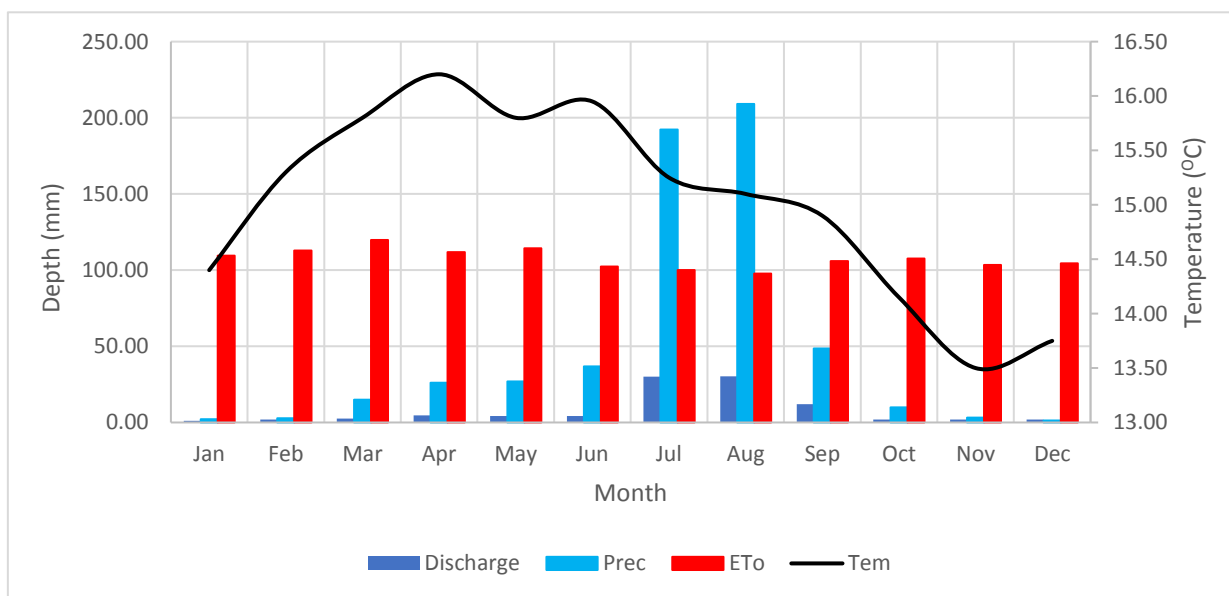


Figure 2. Mean monthly precipitation (Prec), temperature (Temp), evapotranspiration (ET0), and discharge

Table 1. Results of Thiessen polygon method's analysis of the stations' contributions to each catchment's rainfall

Stations' contributions of rainfall to each catchment using Thiessen polygon method (Weightage %)		AbiAdi	Adigrat	Adigudem	Dengolat	E/hamus	Hawzen	H/Selam	Mekelle AP	Mekelle Ob	Samre	Mukro
S/N	Catchments											
1	Siluh		13			17	33	5		5		27
2	Genfel					22	3			5		70
3	Agulai								6	30		64
4	Tahtay Ghba	31		3	10			16	12	14	13	

2.2 Sources and description of the data

The most important data required are (i) streamflow and in-situ precipitation (ii) climate data: CFSR temperature, wind speed, cloudiness fraction and relative humidity, (iii) spatial data: DEM, land use/cover (LULC), and the depth of the soil layer for the model's calibration and validation. Additionally, it is vital to possess information on geographic latitude (centroid).

2.2.1 Hydrometeorological Input Data

The average annual precipitation depth in the subbasin was determined using the Thiessen polygonal method, as shown in Table 1. The weighted average of each station for the six catchments was established in accordance with flow monitoring stations in order to construct a hydrological model. Figure 5 presents the average monthly data for temperature (Temp), evapotranspiration (ET₀), precipitation (Prec), and discharge input data were offered by the Ethiopian Meteorological Service Agency (NMA) and Ministry of Water and Energy (MWE) respectively. These data were reviewed and filtered for consistency and quality [39]. The monthly relative humidity, wind speed, and cloudiness friction were also offered by Ethiopian Meteorological Service Agency (NMA) for several years. In order to read the average monthly values from a CSV file into WEAP as a time series expression, they were repeated for each corresponding month.

2.2.2 Static Input Data DEM, Soil, and Land Use

Based on an SRTM Digital Elevation Model (DEM) with a 30 m resolution, the watershed delineation and streamflow networks extraction were carried out. Additional discretization of the Subbasin into the following essential computational units: land use and cover data for year 1990, 2000, 2010 and 2020 were collected from previous studies [32]. The Ghba subbasin's LULC is distinguished by extreme land degradation brought on by overgrazing, deforestation, and farming on the topographically challenging terrain. Rain-fed agriculture predominated in the research area

during the designated time periods, with the principal crops being pulses, barley, teff, sorghum, wheat, and maize. Shrubs, bare ground, wood, grassland, plantations, residential areas, forests, and water were next in line (Figure 3). Nevertheless, the previous 10–15 years have seen a substantial expansion in small-scale irrigation systems for irrigated agriculture due to the government's millennium development plan across the subbasin's eastern, central, and northern regions [70–72].

The dominant soil types identified in the Ghba subbasin includes, Lithic Leptosol (40.8%), Eutric Leptosol (25.7%) on the steep lands, Vertic Cambisol (21.1%), Haplic Lixisol (8.3%), Eutric Cambisol (2.3%) and Chromic cambisol (1.8%) (Fig 2.5) this soil profile or map was verified Using the description of 141 profile pits, and 1381 soil auguring [67]. A soil map used for the current study was developed by field-based/supervised method in which a demonstrative sub-catchment was first mapped and all this data was combined in to a comprehensive map at 1: 2500,000 scale taking into consideration the complexity of the topography this method was preferred over digital or predictive soil mapping [66, 67, 73]. Nyssen, Tielens [67] suggested a new methodology to develop a soil profile of the research topic by using the Aster DEM, SPOT images (January 2005), the ground collected soil data map, Landsat images (February 2003), SPOT images (January 2005) and aerial photographs (January 1994), earlier baseline soil data for the research topic was accessed primarily small-scale maps based on FAO [74, 75] at 1:1,000,000 scale, derived maps include the e-SOTER map [76] and the corresponding sheets in the Soil Atlas of Africa (Figure 4).

2.3 Model description

Through simulating probable interactions between multiple elements, WEAP is a semi-distributed modelling system used to model hydrologic time series characteristics [77]. The model evaluates the hydrologic behaviour within a subbasin or catchment characteristics. The selected model structure of the

hydrology component soil moisture method is a rainfall-runoff method-based lumped continuous model [78]. This assumes that a two-layer, one-dimensional soil moisture dynamic functioning system will be used to divide water into the hydrological processes mass

balance (Deep percolation, ET, sub-surface runoff/interflow, and surface runoff) at the rootzone level for the Ghba subbasin as expressed in Eq. 1. The corresponding conceptual model diagram is seen in Figure 5.

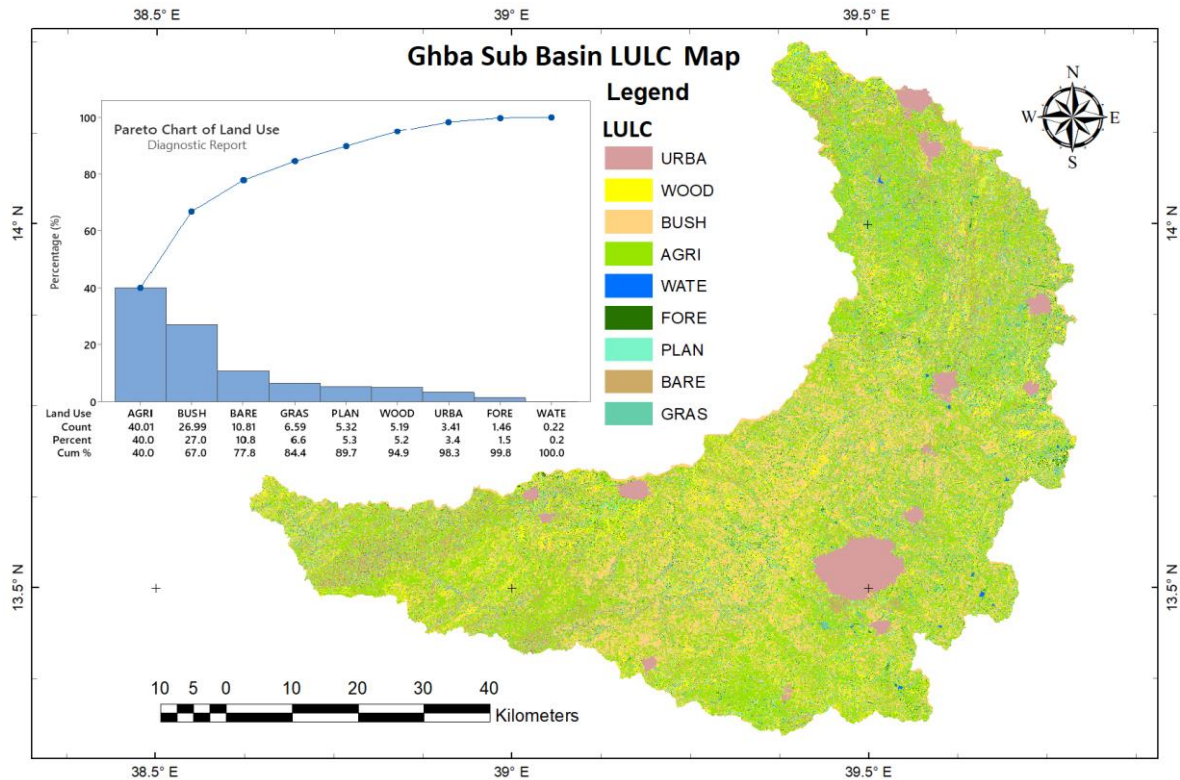


Figure 3. Ghba Subbasin land use and cover map

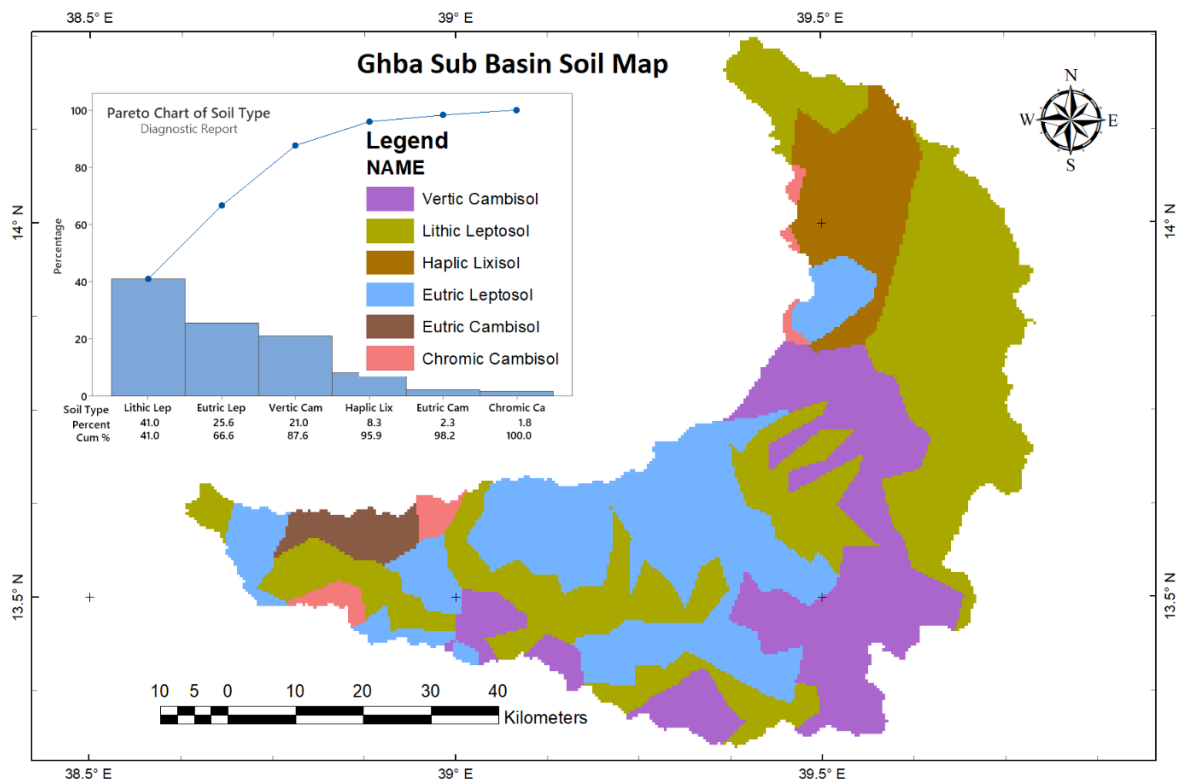


Figure 4. Significant types of soil in the Ghba subbasin

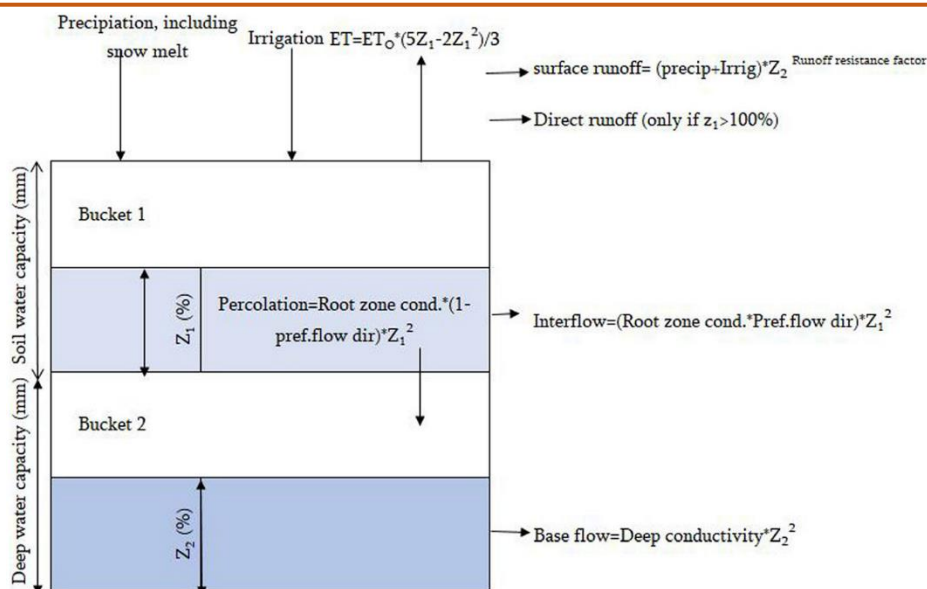


Figure 5. Schematization of the varied soil moisture processes and fluxes model structure of WEAP hydrology

Nine distinct types of land use/cover (j) make up the Giba subbasin, and their combined total area equals 100% of the subbasin's total area. The LULC (j) values with analogous property from each catchment area are added while dropping ET from the system and connecting the base flow, surface runoff and interflow to a river network. It computes a water balance for each distinct value region, j of N. The subbasin unit's deep percolation may be disseminated to a body of surface water as base flow or immediately to groundwater storage when proper connection between the subbasin groundwater node and a unit node are built.

$$Rd_j \frac{dz_{1,j}}{dt} = p_e(t) - ET_o(t)K_{c,j}(t) \left(\frac{5Z_{1,j} - 2Z_{1,j}^2}{3} \right) - p_e(t)Z_{1,j}^{RRF_j} - f_j k_{s,j} Z_{1,j}^2 - (1 - f_j)K_{s,j}Z_{1,j}^2 \quad (1)$$

$Z_1, j, 0, 1$ represents the proportion of the total amount of actual water stored in the root zone's layers of the dimensionless land use j that is stored in the soil. Rd_j is the ability of soil to retain water for use j [mm], P_e is actual precipitation [mm], $ET_o(t)$ i.e., reference evapotranspiration [mm/day], the coefficient of land usage, j for crops $K_{c,j}$; j is land cover and use factors that affect runoff resistance RRF_j , $P_e(t)Z_{1,j}^{RRF_j}$ is runoff from the surface, $f_j k_{s,j}Z_{1,j}^2$ is interconnection to the top land use layer j, f_j is the area's topography, soil, and partitioning coefficient in relation to the type of land cover, j, that separates the horizontal flow f_j and vertical $(1 - f_j)$ flows, and $K_{s,j}$ (mm/time) is land uses' saturable hydraulic conductivity (j) root zone layer.

In Eq. 1, The Penman-Monteith equation is modified to account for a standard crop of grass that is 0.12 meters tall and surfaces with a resistance of 61 s/m to determine the reference ET, which is represented by the second term. With Eq. 1 still in place, the $k_{c,j}$ is for each partial land cover, the crop/plant coefficient. RRF_j , the land cover's capacity to resist runoff, is used to indicate surface runoff in the third term. Less surface runoff results from RRF_j values that are higher. While the 4th

term is interflow and 5th term deep percolation. where the parameter $k_{s,j}$ is the root zone's estimated saturation conductivity (mm/time), and f_j is a partitioning factor connected to soil, type of land cover, and topography that separates water fractionally in both directions horizontal and vertical. Eq. 2 reflects each sub catchment's interflow and overall surface runoff (RT) at time t.

$$RT(t) = \sum_{j=1}^N A_j P_e(t) Z_{1,j}^{RRF_j} \quad (1)$$

According to Eq. 3, the basin's total interflow is determined by adding up each sub catchment at a specific time t.

$$IF(t) = \sum_{j=1}^N A_j f_j K_{s,j} Z_{1,j}^2 \quad (2)$$

The ground-water recharge (R) After becoming familiar with the model and building links for runoff and infiltration between groundwater node and the watershed unit, one can estimate the volume of an alluvial aquifer over time using Eq. 4.

$$R = \sum_{j=1}^N A_j (1 - f_j) K_{s,j} Z_{1,j}^2 \quad (3)$$

For cases where a groundwater node and a catchment do not have a return flow link established, the base flow coming from the second vessel is calculated using Eq. 5.

$$S_{max} \frac{dz_2}{dt} = \left(\sum_{j=1}^N (1 - f_j) K_{s,j} Z_{1,j}^2 \right) - K_{s,2} Z_{2,j}^2 \quad (4)$$

Where S_{max} , the inflow into this storage, is profound percolation coming from the top storage described in Eq. 5, and $K_{s,2}$, the lower storage's saturated conductivity, it is provided as one figure to the subbasin, hereafter does not have a subscript, j, is measured in millimetres per time. The reference evapotranspiration (RE), crop coefficient (K_c), and soil water content within the root zone of the modelling unit are also used to estimate actual evapotranspiration (ET).

$$ET = ET_o \times K_c (5Z_1 - 2Z_1^2) / 3 \quad (5)$$

When there is enough water on the reference surface to satisfy atmospheric evaporation needs, ET_0 is widely understood to represent the water's volume that would evaporate into the atmosphere from a terrestrial surface. The ET_0 estimation uses conventional Solar radiation data from climatology (sunlight), wind speed, humidity, and air temperature over a broad expanse of green grass shadowing the ground but not dry (Allen et al.1998). Eq. 7 provides the Penman-Monteith method's expression for estimating ET_0 .

$$ET_0 = \frac{0.408\Delta(R_n - G) + \gamma \frac{900}{T + 273} u_2 (e_s - e_a)}{\Delta + \gamma(1 + 0.34u_2)} \quad (6)$$

Where, the reference evapotranspiration is ET_0 (mm/day). , R_n is the surface's overall radiation of the crop (MJ/m²day), G density of soil heat flux (MJ/m²day), T is average at 2 meters, the daily air temperature in height (°C), u_2 is the 2 meter height wind speed (m /s), e_s is the vapor pressure of saturation (kPa), Actual vapor pressure is given by e_a (kPa), $e_s - e_a$ is shortfall in vapor pressure at saturation (kPa) , Δ is vapor pressure slope curve (kPa /°C), while γ described as psychrometric constant (kPa/°C).

2.4 Model Schematization

The above input data for the Ghba river hydrology was schematized as follows: First six catchments for each station were delineated using GIS, second the centroid of each catchment was calculated then the catchment tab in the WEAP modeling system were dragged and put at each centroid for each catchment, third an infiltration/runoff link were dragged from each catchment centroid to the gaging station (Figure 6). Then, the model was ready for characterization.

2.5 Validation and calibration

The primary goal of model calibration was to generate a list of parameters suitable for the basin or subbasin in order to accurately estimate and depict the system's hydrology at the gauging stations [79, 80].

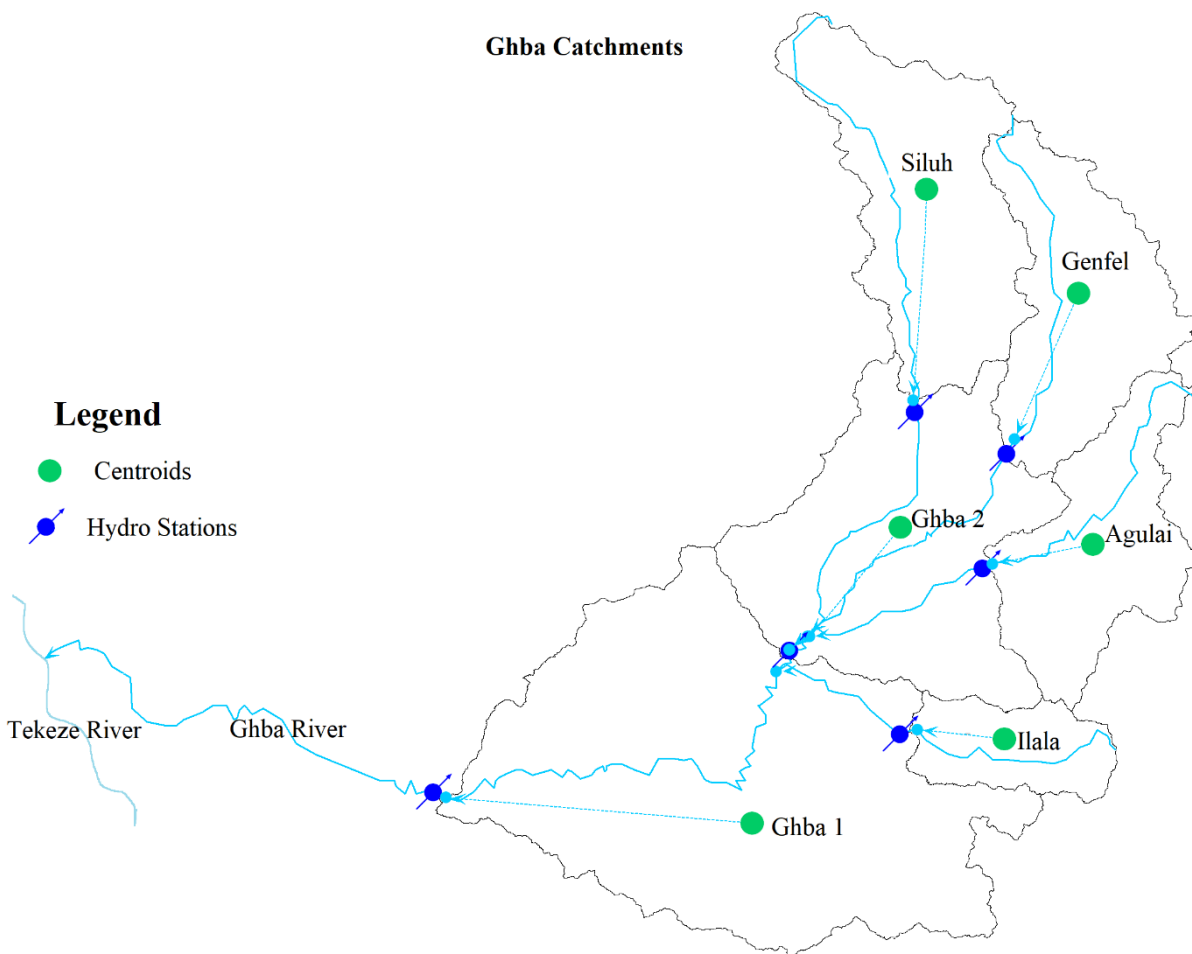


Figure 6. Schematic map of WEAP hydrological model development for six catchments and infiltration/runoff links of Ghba subbasin.

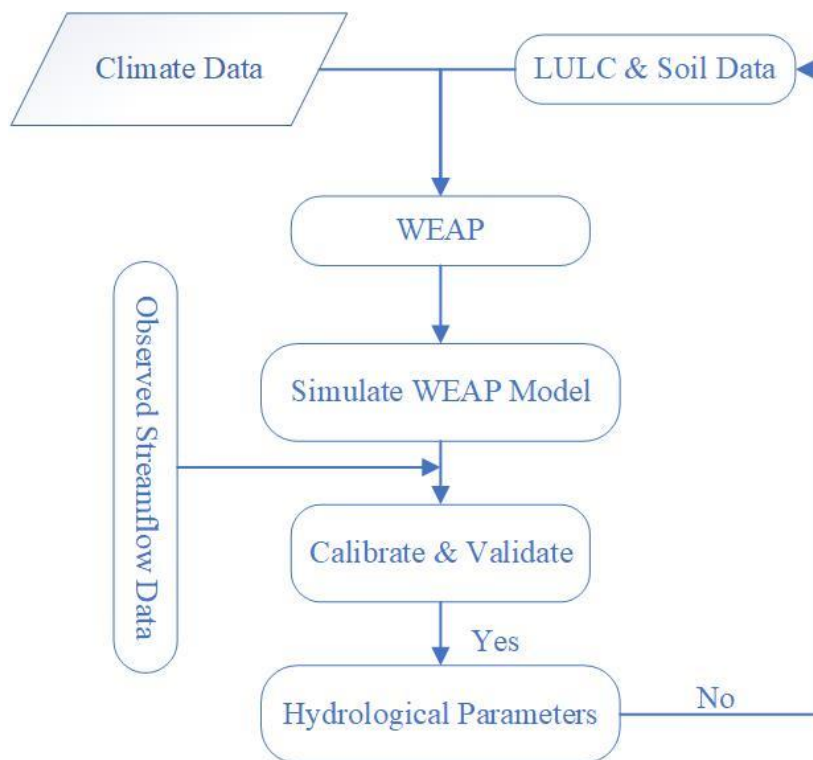


Figure 7. Schematic diagram of hydrologic model procedure polygon

The model calibration techniques can be achieved either by manual or automatic calibration, hence the automatic calibration needs to give threshold of parameters that represents to the system. Otherwise, the result will be vague [81]. To reduce the discrepancy between simulated and observed values, it is highly recommended to undertake the sensitivity studies prior to calibration. Calibration and validation procedures will proceed more quickly as a result [82, 83]. The WEAP model with soil moisture method model structure includes Seven factors relating to soil and land usage [84, 85] this helps to recalibrate the hydrologic model better agreement with the observed once. These are: coefficient of crop (Kc), soil water capacity (Sw), deep water capacity (Dw), factor for runoff resistance (RRF), the root zone's conduciveness (Ks), deep zone conductivity (Ka), preferred flow direction (f) and first storage percentage at the start of simulating the top soil layer (Z1) and the lower soil layer's lower soil layer's initial storage fraction (Z2).

To simulate the streamflow outputs of the hydrological model a Weather information for each month was used, including average temperature, rainfall, relative humidity, sunlight hours, wind speed, land usage, and soil properties. The model's manual calibration for estimating LULC and soil-related parameters until a good agreement is between the simulated and measured streamflow's. A flowchart of the hydrologic model WEAP procedure is shown in Figure 7.

Finally, yet importantly, Modelling basin/subbasin hydrologic conditions is the most important aspect to the use of hydrologic models. As a result, the model validation procedure is vital to

determine the viability of a model for simulating a basin's or subbasin's hydrologic response under conditions different from those employed throughout the calibration period [86].

2.6 Model measures for performance evaluation

Results of model validation and calibration are always assessed by model performance indices using various techniques mainly the statistical methods are common [87], and other technics like combined plots Utilizing error bars, when compared to the monthly and average month hydrographs from the modelling period and observations [88]. The following statistical and combined graphic techniques were employed to assess how well a model's outputs fit a subbasin of the Gbba hydrology based on ground measurements: The correlation between two variables (R²) Eq. 8, the Nash-Sutcliffe efficiency coefficient (NSE), Eq. 9, the agreement index (IA), Eq. 10, the error, root mean square (RMSE), Eq. 11, the ratio of the observations' standard deviation (RSR), Eq. 12, and Eq. 13, which calculates the percentage of bias (PBIAS).

$$R^2 = \frac{(\sum [x_i - \bar{x}][y_i - \bar{y}])^2}{\sum (x_i - \bar{x})^2 \sum (y_i - \bar{y})^2} \tag{7}$$

$$NSE = 1 - \frac{\sum_{i=1}^n (x_i - y_i)^2}{\sum_{i=1}^n (x_i - \bar{x})^2} \tag{8}$$

$$IA = 1 - \frac{\sum_{i=1}^n (x_i - y_i)^2}{\sum_{i=1}^n (|y_i - \bar{y}| - |x_i - \bar{x}|)^2} \tag{9}$$

$$RMSE = \sqrt{\frac{\sum_{i=1}^n (x_i - y_i)^2}{n}} \tag{10}$$

$$RSR = \frac{\sqrt{\sum_{i=1}^n (X_i - Y_i)^2}}{\sqrt{\sum_{i=1}^n (X_i - \bar{Y})^2}} \tag{11}$$

$$PBIAS = \left[\frac{(\sum y_i - \sum x_i)}{(\sum x_i)} \right] \times 100 \tag{12}$$

Where, respectively, X_i , Y_i , \bar{X} , \bar{Y} ; and n represent the i^{th} monthly discharge measurements, the i^{th} monthly discharge simulation data, the average of the monthly discharge measurements, the average of the monthly discharge simulation data, and data on all observations combined. The model indices chosen for the current investigation have been utilized successfully to large-scale WEAP model application [59, 89-92].

Utilizing information from the model simulation, the effectiveness of the model's efficiency was confirmed versus measured streamflow data. According to many studies [93, 94, 95], the values of PBIS ranges from 0 to $\pm 100\%$, that are less than 25% are acceptable as the value decreases it shows reduced error variance. In general, the values of model indices can be described as follows: NSE values vary from $-\infty$ and 1, R^2 , IA and RSR ranges from 0 to 1, RMSE value depends on the dataset No matter if a particular RMSE score is "low," and the lower result is the better agreement. Table 2 summarizes the total model performance rating.

2.7 Evaluation of Total Water Storage, Water Balance, and Water Yield

Based on the results of the WEAP model, an evaluation of the watershed's long-term average water balances was done. The following equation is used to forecast the catchment's water yield.

$$WT = Q_s + Q_{La} + Q_{Gw} - Q_{Tloss} \tag{13}$$

where

- WY is water yield
- Q_s is the surface runoff;
- Q_{La} is the lateral flow;

- Q_{Gw} is the contribution of groundwater to streamflow by percolation;
- $Q_{Total\ loss}$ is the transmission loss.

In order to determine if the catchment has a surplus or deficit of water for the given month, total water storage (WS) is additionally assessed. The release or storage of water will depend on the month. Runoff and Actual Evapotranspiration (AET) are subtracted from precipitation to determine water storage. To assess the basin's water storage condition, two circumstances are taken into consideration:

- Case one if Precipitation > WY + AET (Positive storage), Infiltration and storage of extra water as groundwater storage and soil moisture.
- Case two if Precipitation < WY + AET (Negative storage), indicating that any water shortage will be made up for by the storage.

3. Results and discussion

3.1 Model calibration and validation

According the model developed for the Ghba subbasin hydrology, A higher agreement was seen in the hydrographs of the monthly streamflow simulation and the actual data model indices over the validation and calibration periods. The model's efficacy in replicating streamflow was assessed using the model indices listed in Table 3 for R2, NSE, IA, RSR, and PBIAS. During the stages of validation and calibration, the Ghba River's monthly runoff, both real and simulated at six stations is shown in Figures 8 and 9. The optimum model parameters within the threshold of the catchment characteristics is estimated and shown in Table 4. Furthermore, Figure 10's depiction of the average simulated and measured streamflow for each month at Ghba 1 station reveals a greater correlation between mean monthly simulated and measured streamflow and thus, The R2, NSE, and IA values for the calibration time were 0.93, 0.94, and 0.96, whereas those for the validation time were 0.80, 0.81, and 0.91.

Table 2. Evaluation criteria for the quality indicators of model output Vs measured data

Performance rating	R2	NSE	IA	RSR	PBIAS (%)
Very good	$0.75 < R^2 \leq 1$	$0.75 < NSE \leq 1$	$0.75 < AI \leq 1$	$0 \leq RSR \leq 0.5$	$PBIAS < \pm 10$
Good	$0.65 < R^2 \leq 0.75$	$0.65 < NSE \leq 0.75$	$0.65 < AI \leq 0.75$	$0.5 \leq RSR \leq 0.6$	$\pm 10 \leq PBIAS < \pm 15$
Satisfactory	$0.5 < R^2 \leq 0.65$	$0.5 < NSE \leq 0.65$	$0.5 < AI \leq 0.65$	$0.6 \leq RSR \leq 0.7$	$\pm 15 \leq PBIAS < \pm 25$
Unsatisfactory	$R^2 \leq 0.5$	$NSE \leq 0.5$	$AI \leq 0.5$	$RSR > 0.7$	$PBIAS \geq \pm 25$

Table 3. Model calibration and validation performance metrics at the monthly scale

S/N	Catchment	Calibration					Validation				
		R2	NSE	IA	RSR	PBIAS (%)	R2	NSE	IA	RSR	PBIAS (%)
1	Siluh	0.88	0.87	0.84	0.95	7.5	0.82	0.81	0.81	0.83	10
2	Genfel	0.85	0.86	0.81	0.91	8.1	0.80	0.82	0.82	0.79	11
3	Agulai	0.83	0.83	0.83	0.88	6.8	0.81	0.83	0.81	0.81	9
4	Illala	0.87	0.84	0.88	0.85	7	0.83	0.82	0.78	0.82	9.7
5	Ghba 2	0.81	0.81	0.85	0.91	7.8	0.78	0.81	0.77	0.81	12
6	Ghba 1	0.82	0.82	0.8	0.87	9	0.78	0.81	0.7	0.8	11.5

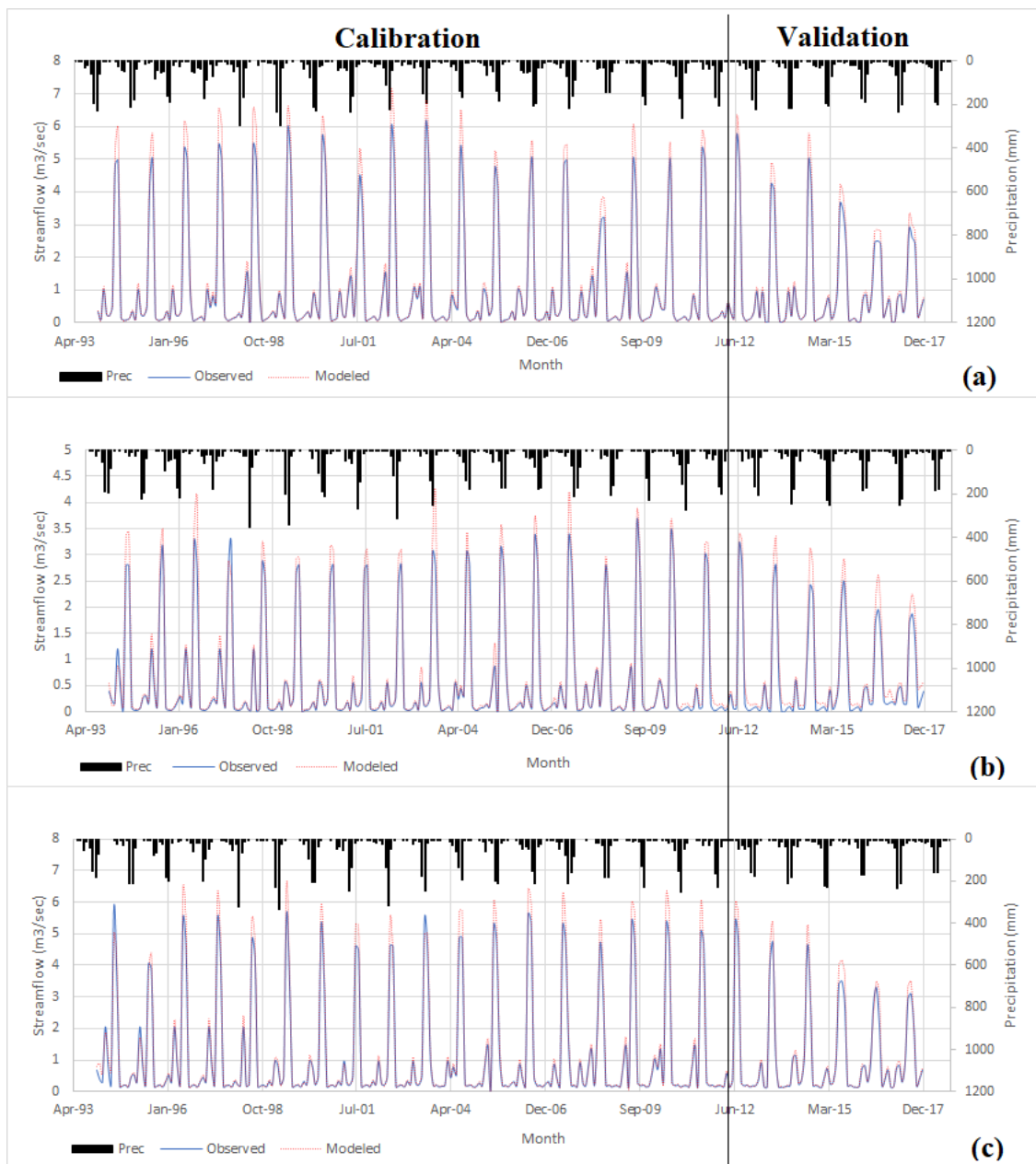


Figure 8 Calibration and validation Siluh (a), Genfel (b) and Agulai (c) hydro stations of WEAP model

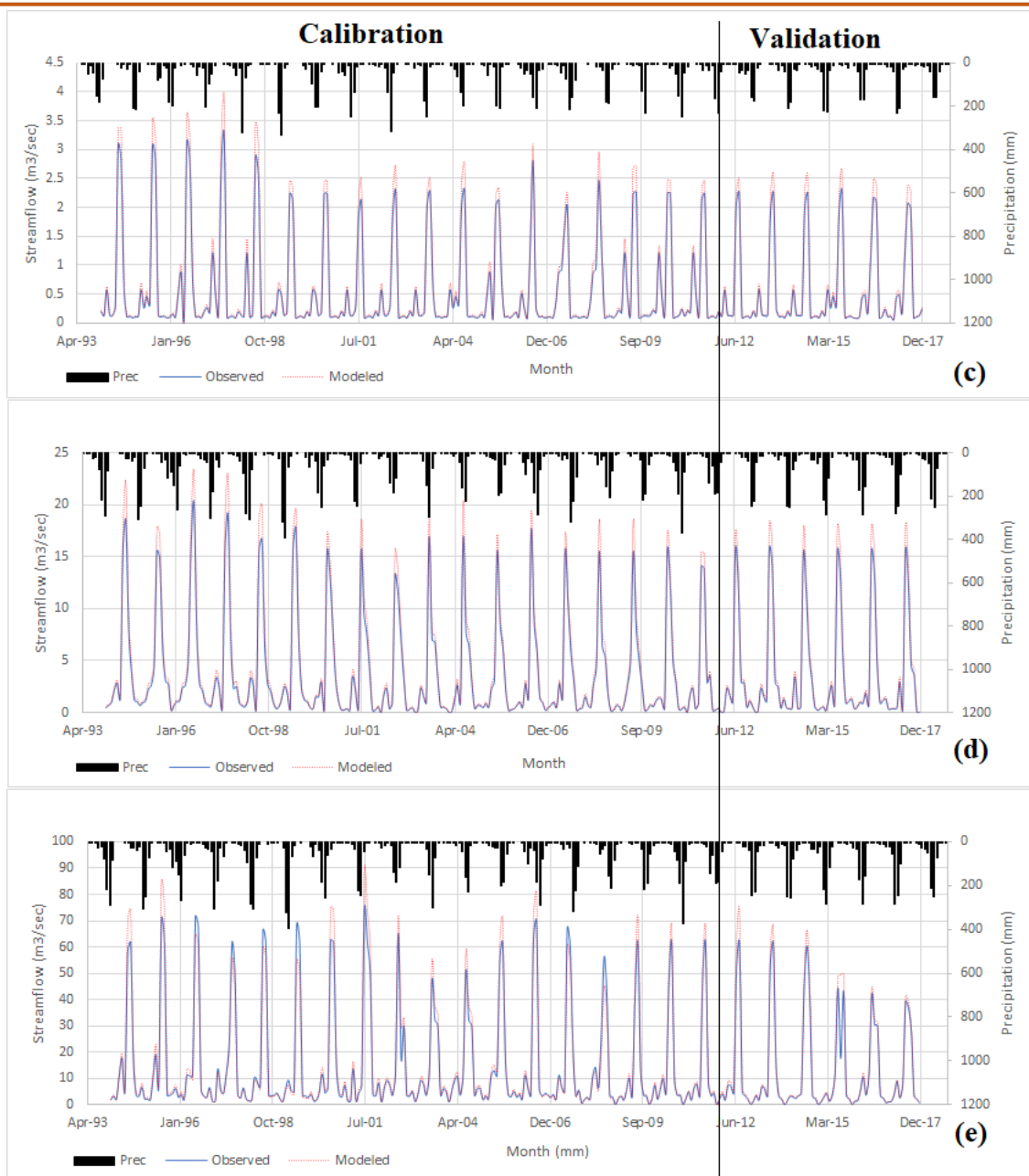


Figure 9. Calibration and validation Ilala (c), Ghba 2 (d) and Ghba 1 (e) hydro stations of WEAP model

Table 4. Range of computed parameter values for the Ghba River subbasin

Parameters	Definition	Range in values
Kc	Crop coefficient	0.35 -1.15
SWC	Effective soil water capacity of the upper layer [11]	550
DWC	Effective soil water capacity of the lower layer [11]	300
RRF	Runoff resistance factor	2.5 - 405
RZC	Root zone rate of conductivity at full saturation (mm/month)	0.5 -185
DC	Rate of conductivity of deep layer at full saturation (mm/month)	4 - 28
PF	Preferred flow direction	0.68
Z ₁	Initial storage fraction of upper layer at the beginning of the simulation (%)	25 - 55
Z ₂	Initial storage fraction of lower layer at the beginning of the simulation (%)	68

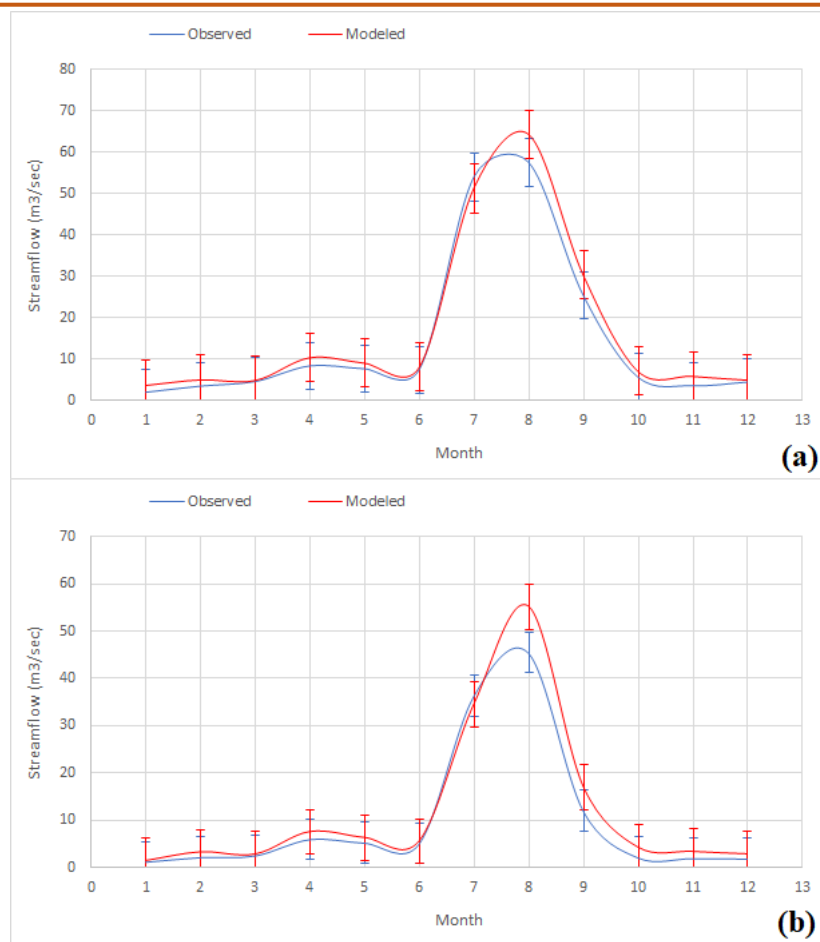


Figure 10. For the calibration (a) and validation (b) periods, the average monthly hydrograph of the Ghba River at the Ghba 1 gauging station shows simulated and measured flows; the blue line and red line error bars, respectively, show the standard errors of monthly simulated and measured flows.

Regarding recapturing the general streamflow features, the model was generally able to retain a fairly good agreement. Additionally, prior research has demonstrated the WEAP hydrologic model's capability to reveal Processes of catchment hydrology in another area of the world with very good agreement of the model criteria indices, such as in evaluating potential effects of land-use as well as climate change that effect on potable water, irrigation, and animal husbandry water supply [62, 89, 92, 96, 97, 98].

3.2 Hydrological processes

3.2.1 Annual Water Balance Components

The sub basin's sole source of water inflow is precipitation, which totals 650 mm annually [2]. The global precipitation is potentially used by evapotranspiration also being highly uncertain and difficult to estimate the amount accurately [99, 100]. Precipitation estimates play a vital role in climate change research as well as water resource management and allocation, agriculture, and hydrological predictions. The long-term hydrological analysis of the four catchments of the current study is summarized in Table 5. This analysis is based on monthly data and provides an overview of

the hydrological conditions in the catchments. The current study showed that the average ET loss for four watersheds was 406.05 mm/year. The other output of the subbasin water balance model is the runoff or streamflow. To calculate this the surface runoff, baseflow, and interflow are added together these are, 70 mm/year, 34.33 mm/year, and 75.61 mm/year respectively. Thus, evapotranspiration loss accounts for 63.4% of the total precipitation, that is, 640.12 mm. This outcome is in line with the research by Gebremedhin [101] Research demonstrated that ET consumes 60 to 65 percent of precipitation in the subbasin of Ghba. Evapotranspiration (ET) was higher in the drier months than precipitation. As opposed to that, during the wet and rainy seasons, ET was lower than Precipitation amounts, and in September and February, it was about equal. The Ghba sub basin's water balance was investigated in the current study. It was discovered that 28.3 percent of precipitation turns into runoff from streams, which is composed of 11.8 percent interflow, 5.4 percent baseflow, and 11.1 percent surface runoff, respectively. Another study by Aredehey, Mezgebu [44] Using the SWAT modeling system demonstrates that the current study is accurate. while, the study by Gebremicael [4] in contrast to the present study, streamflow model findings

using the Wflow PCRaster model indicate greater values.

Table 6 demonstrates that the wettest year is when all of the yearly water balance components with higher values are observed (1986), in contrast, the contribution of the water balance components to the water budget declined noticeably in dry years (1984, 1990, 1992, 1993, 1994, 2001, 2002, 2003, 2004, 2005, 2008, 2009, and 2012), when the rainfall was below average. The same pattern was observed in earlier research conducted in the headwaters of the Nile basin [87, 101, 102], where the contribution of the various elements of the water balance decreased as precipitation decreases.

The catchments for their peak and lower potential of providing water balance components, 1986 and 2004 were deemed critical years, respectively. It is noted that in most years surface runoff decreases as rainfall remains almost similar (Figure 11), this is due to soil and water conservation interventions and change in catchment characteristics [101].

The watershed receives 640.12 mm of rainfall annually, according to the water balance for the

simulated period (1983–2017). Baseflow and actual evapotranspiration made up the majority and a small portion of the annual water budget, respectively. The actual evapotranspiration, interflow, baseflow, surface runoff, and groundwater recharge (percolation) accounting for 63.4%, 11.8%, 5.4%, 11.1%, and 8.3% of the catchment's total water supply, respectively.

According to the estimate of the water balance, evapotranspiration accounts for 63.4 percent of the catchment's yearly precipitation that is returned to the atmosphere. A significant portion of the catchment's water balance is accounted for by evapotranspiration. In especially in the study area, past research carried out in Ethiopia lends confirmation to the findings of the current study. A study by [57, 68, 101] in the Blue Nile headwaters showed that about 48 up to 60 % of the total rainfall is AET. A study on regional ground water modelling on Ghba river using MODFLOW by [103] showed that about 8 up to 10 % of precipitation is the only source of recharge for groundwater recharge. Figure 12 shows the spatial distribution of the elements of the water balance.

Table 2. Hydrologic components' avg. monthly estimated depth (mm) in the Ghba subbasin

Month	Prec	AET	Baseflow	Interflow	Surface runoff	Runoff
Jan	0.13	21.85	0.40	0.00	0.00	0.40
Feb	4.6	20.5	0.40	0.54	0.50	1.44
Mar	7.83	20.2	0.47	0.94	0.87	2.27
Apr	25	33.4	1.26	2.96	2.78	6.99
May	15.55	35.2	0.79	1.84	1.73	4.36
Jun	71.01	39.1	3.57	8.40	7.90	19.87
Jul	196	39.1	9.88	23.15	21.78	54.80
Aug	240	47.2	12.11	28.34	26.65	67.10
Sep	80	46.1	4.04	9.45	8.87	22.35
Oct	0	49.2	0.54	0.00	0.00	0.54
Nov	0	35.1	0.47	0.00	0.00	0.47
Dec	0	19.1	0.40	0.00	0.00	0.40
Sum	640.12	406.05	34.33	75.61	71.07	181.00
Min	0.00	19.10	0.40	0.00	0.00	0.40
Max	240.00	49.20	12.11	28.34	26.65	67.10
Mean	53.34	33.84	2.86	6.30	5.92	15.08
%	100.0	63.4	5.4	11.8	11.1	28.3

Table 3 Mean annual Water Balance components of Ghba subbasin (1983–2017).

Year	Precipitation	AET	Baseflow	Interflow	Surface runoff	Runoff	Percolation	Water yield
1983	654	415	35	77	73	185	54	239
1984	580	368	31	68	64	164	48	212
1985	658	417	36	78	73	186	55	241
1986	784	497	42	93	87	222	65	287

1987	669	424	36	79	74	189	56	245
1988	737	468	40	87	82	209	61	270
1989	653	414	35	77	73	185	54	239
1990	519	329	28	61	58	147	43	190
1991	692	439	37	82	77	196	57	253
1992	569	361	31	67	63	161	47	208
1993	621	394	34	73	69	176	52	227
1994	643	408	35	76	71	182	53	235
1995	676	429	37	80	75	191	56	247
1996	720	456	39	85	80	204	60	263
1997	605	383	33	71	67	171	50	221
1998	695	441	38	82	77	197	58	254
1999	740	469	40	87	82	209	61	271
2000	640	406	35	75	71	181	53	234
2001	599	380	32	71	66	169	50	219
2002	503	319	27	59	56	142	42	184
2003	529	335	29	62	59	150	44	194
2004	469	297	25	55	52	133	39	172
2005	509	323	27	60	56	144	42	186
2006	717	454	39	85	80	203	59	262
2007	650	412	35	77	72	184	54	238
2008	550	349	30	65	61	156	46	201
2009	500	317	27	59	56	142	42	183
2010	732	464	40	86	81	207	61	268
2011	606	384	33	72	67	171	50	222
2012	584	370	32	69	65	165	48	214
2013	646	409	35	76	72	183	54	236
2014	711	451	38	84	79	201	59	260
2015	630	399	34	74	70	178	52	231
2016	711	451	38	84	79	201	59	260
2017	622	394	34	73	69	176	52	227

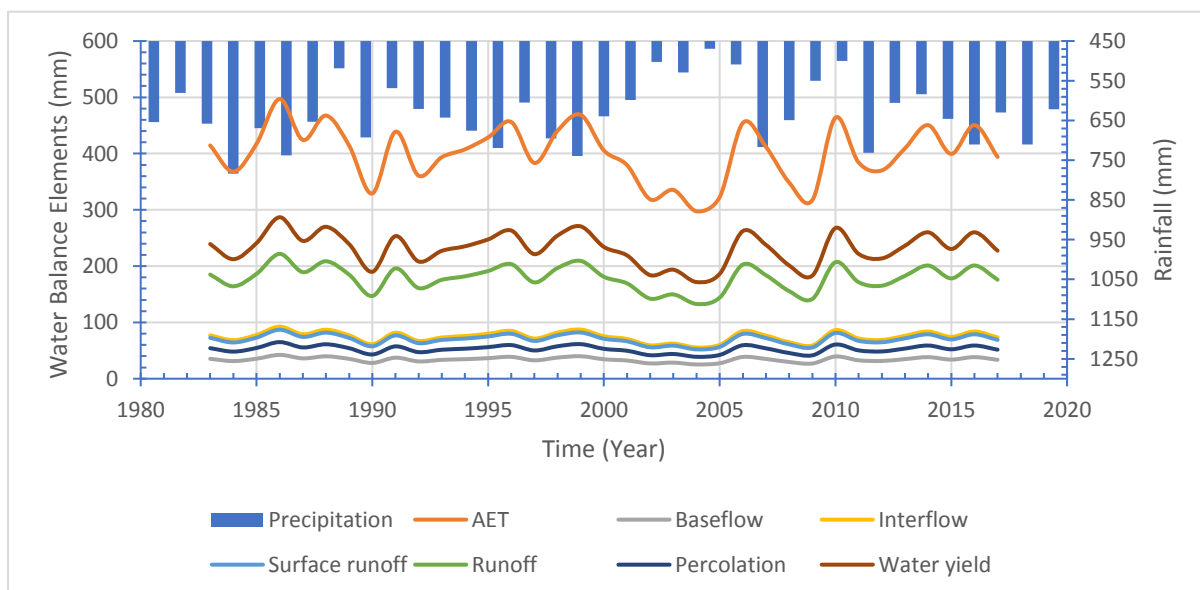


Figure 11. Distribution of the simulated water balance components' mean annual values from 1983 to 2017

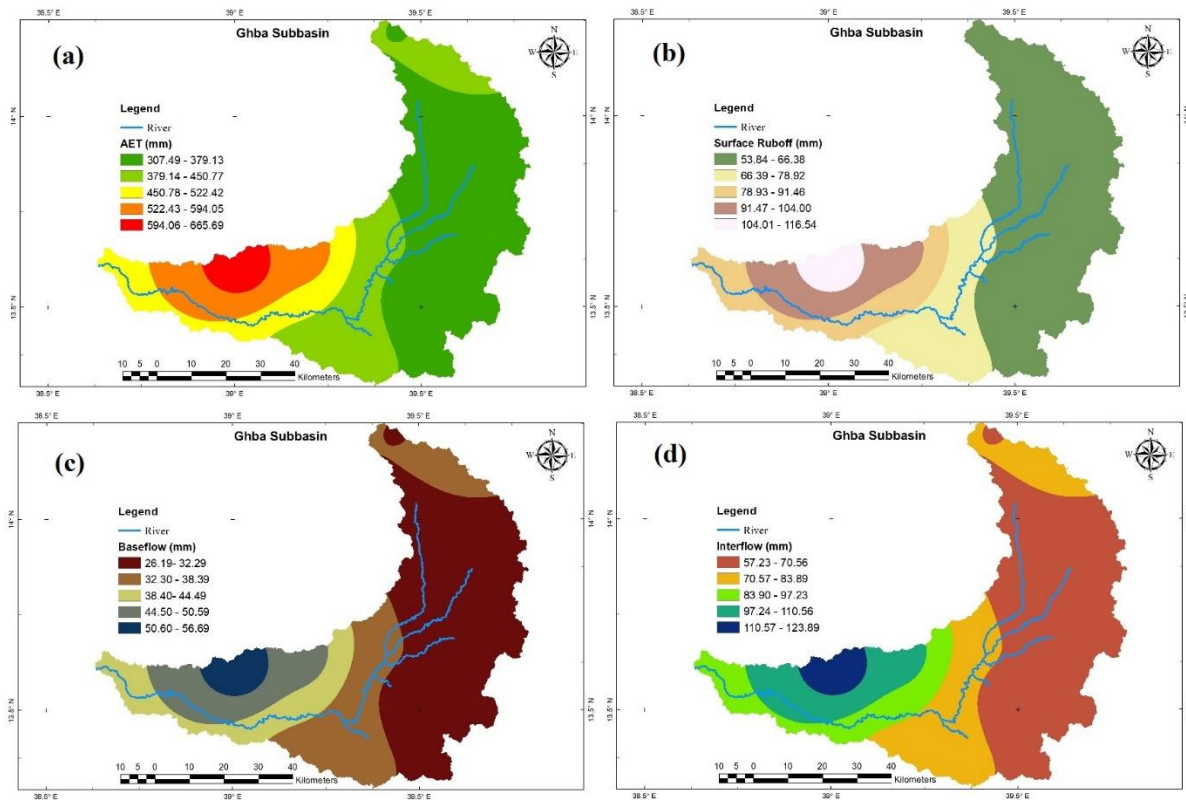


Figure 12 Distribution of the average yearly water balance components in space, Actual evapotranspiration (a), Surface runoff generated (b) Baseflow (c), and Interflow (d).

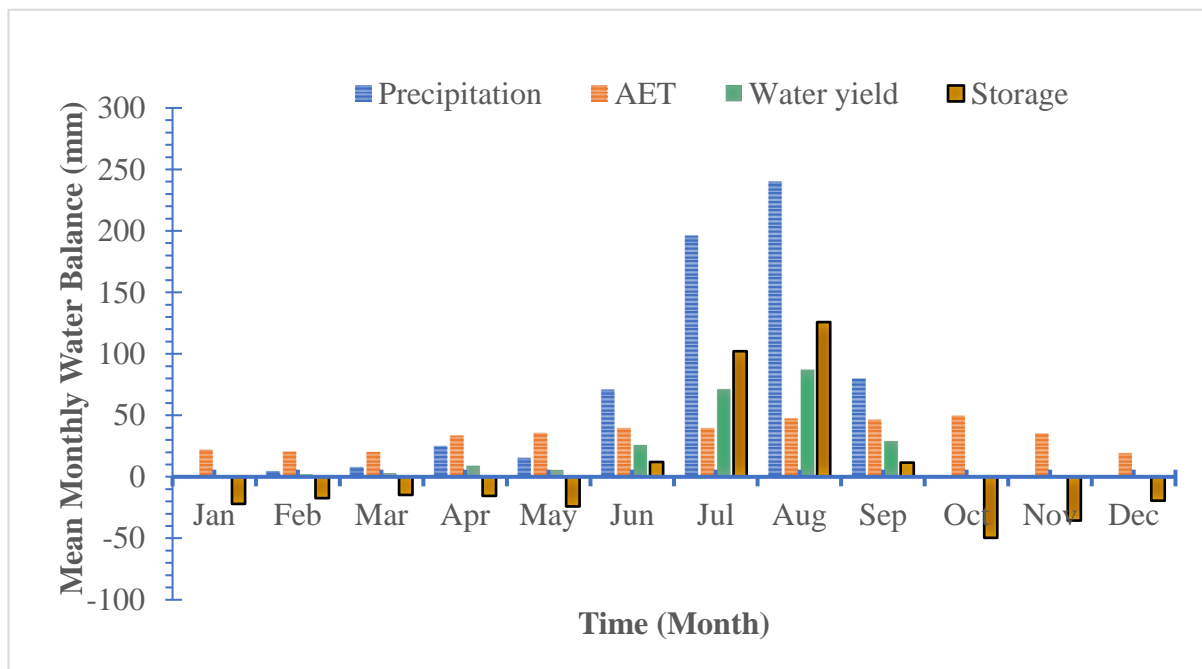


Figure 13 Based on parameters from multivariable calibration, the long-term mean monthly simulated water balance value ranges from 1983 to 2017.

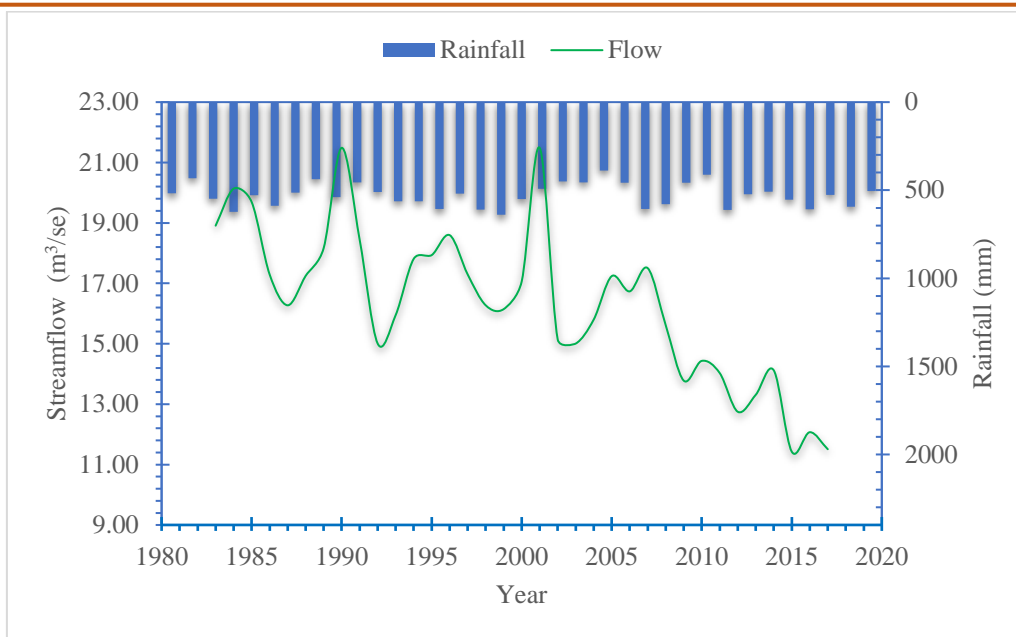


Figure 14 Annual rainfall and streamflow trend

Table 4. Average monthly flows (m³/s) of Ghba subbasin at the outlet (1983–2017) for Q₂₅, Q₅₀ (median), and Q₇₅.

Month	Median Flow (Q ₅₀)	Coefficient of Dispersions (Q ₇₅ – Q ₂₅)/Q ₅₀	Month	Median Flow (Q ₅₀)	Coefficient of Dispersions (Q ₇₅ – Q ₂₅)/Q ₅₀
Jan	1.87	0.45	Jul	53.18	0.41
Feb	3.37	0.67	Aug	53.57	0.19
Mar	4.47	0.81	Sep	21.37	1.05
Apr	8.25	0.56	Oct	3.57	0.05
May	7.57	0.76	Nov	3.47	0.41
Jun	7.30	0.94	Dec	3.31	1.63

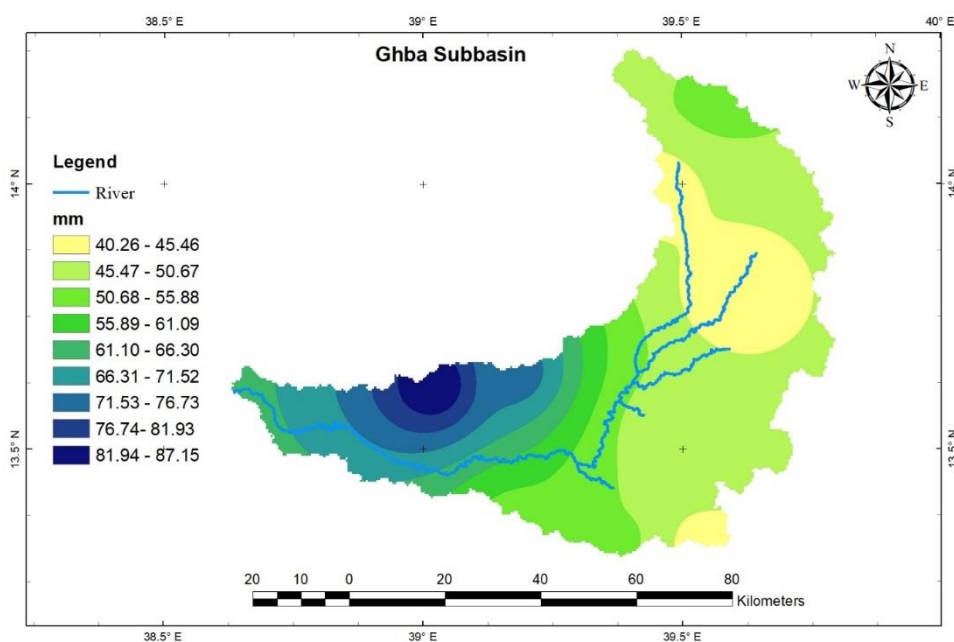


Figure 15 Average annual recharge

3.2.2 Assessment of Total Water Storage and Water Yield

In order to determine the catchment's water yield and storage situation, the monthly water balance was also examined. The water yield makes up all of the total during the main rainy seasons, or kremti (Figure 13).

Surface runoff, groundwater, and lateral flow all have a role in the fluctuation in water supply. Thus, water yield also increased in proportion to an increase in rainfall, following the same trend. Positive storage, or the ability to store water for both the major rainy season and the short rainy season, is achieved by following the rhythm of rainfall and runoff.

This is a result of the rainy seasons' heavy precipitation and low evapotranspiration, in contrast, negative storage was seen in the dry season, and as a result, water that had been stored during the wet seasons was released from the earth and soil to make up for the shortfall.

Maximum positive storage in the ground and soil was seen in July (+102.1 mm/month) and August (+125.7 mm/month), which corresponded to the patterns of precipitation and runoff. The two months with the highest negative storage rates were November (35.57 mm/month) and October (49.74 mm/month). During the dry season, the water that the land had stored during the rainy season will evaporate.

3.3 Overflow Conditions

The annual runoff from the Ghba River was calculated to be 28.3 percent, made up of 20 percent baseflow sustained for the entire year, 41 percent interflow (mostly between June and October), and 39 percent surface runoff (occurring mainly in the months of July, August, and September). These outcomes support the research by Aredehey, Mezgebu [44]. Within the same subbasin, employing the SWAT model, Researchers found that of the overall yearly flow, the interflow accounted for about 60%, the baseflow for about 30%, which sustains the dry season's river runoff, and the surface runoff for 10%. The study by Gebremicael [4] shows that the regeneration of plant cover, which increases interflow and ground water recharge, has been greatly aided by the application of water resource management that is interconnected over the past two decades. Contrarily, catchment factors (such as changes in Geology of watersheds, soil, topography, and geomorphology) might be used to explain why surface runoff contributes less to streamflow.

3.4 Streamflow Conditions

The streamflow does not match the basin's pattern of precipitation, as seen in Figure 14. The annual

streamflow demonstrated a statistically significant decreasing trend, according to the Mann-Kendall trend test ($p < 0.05$).

Figure 14 depicts the simulated lowest and maximum mean annual stream flows at the subbasin outlet, which are 11.43 m³/s (2015) and 21.49 m³/s (2001), respectively. The highest rainy year has the largest flow, and the lowest wet year has the lowest flow (2015). Similar results in terms of time and magnitude were found in earlier research [68].

According to statistics from the subbasin's average monthly flow, the low flow occurred in January with a median flow of 1.78 m³/s and a coefficient of dispersion of 0.45, and High flows occur in July and August, with the median flow in August being 53.57 m³/s and the coefficient of dispersion being 0.19. August, the wettest month, had the small coefficient of dispersion (COD), and December, the driest month, had the highest COD (Table 7).

3.5 Recharge Conditions

Precipitation is the only source of recharge for the Ghba subbasin ground water system [104]. There isn't much actual data on groundwater recharge in the research area, but to demonstrate the model's effectiveness, various regional and local ground water flow studies were evaluated and compared with streamflow simulations assuming a significant link between streamflow and groundwater recharge; this correlation has a significant representation in the WEAP model. As a result, the ground water recharge or percolation was validated with the previous studies.

Based on this information, the simulated model recharge value indicated that percolation accounts for 8.3% of the annual volume of water balance, with mean annual recharge being 53.5 mm and minimum and maximum annual recharge being 40.5 and 87.2 mm. The water balance of the subbasin's annual recharge spatial distribution is depicted in Figure 15.

In addition to this, different studies investigated that the groundwater is anticipated to be extremely shallow in the North-eastern part of the subbasin [104]. Some of these locations have already been identified as having groundwater potential, and they are already being utilized, similar to the Abreha-Atsbeha region; However, the majority of these locations are not yet understood or studied.; So, it's crucial to conduct thorough hydrogeological research in these places to learn more about the potential for groundwater and the presence of irrigable land nearby.

4. Conclusion and Recommendations

The investigation of the water resource potential of the Ghba catchments over the period of 1983 to 2017 was carried out. According to the model's performance

evaluation data, for both the validation and calibration periods, there was an excellent agreement between the monthly streamflow that was measured and simulated at the four catchments' outlets that make up the subbasin. According to the model, the subbasin has the highest percentage of water evaporating into the atmosphere by ET. The rainy season accounts for more over 90% of the yearly overall runoff, with only 10% occurring during the dry and brief rainy seasons. The baseflow is a major factor in determining how much water is available in the Ghba river throughout the year, and anything that modifies the sub basin's hydrologic behaviour may have an impact on the quantity and sustainability of streamflow. One can utilize the model to examine in greater detail how land use and cover dynamics and climate change affect subbasin hydrology, which in turn affects basin water availability. Wasteful use of water resources endangers the ecosystem. The indicated exploitable potential should be the basis for how water resources are used. Therefore, the most crucial component of water resource management efforts is understanding the hydrological processes and employing a robust hydrological model.

The method used in this study proved representative to quantify hydrological responses for an improved water allocation strategy. The development of a water management model in the WEAP modelling framework showed good performance in simulating all hydrological components using available spatial and temporal data. Manual calibration techniques were used to minimize the risks associated with uncertainties and overparameterization. The WEAP model can help to identify how Demand and supply for water are linked, and the ability to improve water resource management and scenario development for water allocation. This study provides a valuable reference for future studies of water allocation plans in complex topographical areas like the Ghba subbasin.

References

- [1] T.G. Gebremicael, M.J. Deitch, H.N. Gancel, A.C. Croteau, G.G. Haile, A.N. Beyene, L. Kumar, Satellite-based rainfall estimates evaluation using a parsimonious hydrological model in the complex climate and topography of the Nile River Catchments, *Atmospheric Research*, 266 (2022) 105939. <https://doi.org/10.1016/j.atmosres.2021.105939>
- [2] M.G. Hiben, A.G. Awoke, A.A. Ashenafi, Estimation of Current Water Use over the Complex Topography of the Nile Basin Headwaters: The Case of Ghba Subbasin, Ethiopia. *Advances in Civil Engineering*, (2022) 7852100. <https://doi.org/10.1155/2022/7852100>
- [3] S.K. Weldegebriel, K.J.S. Yeshitela, Measuring the Semi-Century Ecosystem-Service Value Variation in Mekelle City Region, Northern Ethiopia. 13 (2021) 10015. <https://doi.org/10.3390/su131810015>
- [4] T.G. Gebremicael, (2019) Understanding the impact of human interventions on the hydrology of Nile Basin headwaters, the case of Upper Tekeze catchments, CRC Press, London. <https://doi.org/10.1201/9780367853167>
- [5] O. Tsvetkova, T.O. Randhir, Spatial and temporal uncertainty in climatic impacts on watershed systems, *Science of the Total Environment*, 687 (2019) 618-33. <https://doi.org/10.1016/j.scitotenv.2019.06.141>
- [6] A. Bhaskar, L. Beesley, M.J. Burns, T.D. Fletcher, P. Hamel, C. Oldham, A.H. Roy, Will it rise or will it fall? Managing the complex effects of urbanization on base flow, *Freshwater Science*, 35 (2016) 293-310. <https://doi.org/10.1086/685084>
- [7] Y. Tian, Y. Zheng, B. Wu, X. Wu, J. Liu, C.J.E.M. Zheng, Modeling surface water-groundwater interaction in arid and semi-arid regions with intensive agriculture, *Environmental Modelling & Software*, 63 (2015) 170-84. <https://doi.org/10.1016/j.envsoft.2014.10.011>
- [8] S.J. Burian, C.A. Pomeroy, Urban impacts on the water cycle and potential green infrastructure implications, *Urban Ecosystem Ecology*, 55 (2010) 277-296.
- [9] M.G. Hiben, A.G. Awoke, A.A. Ashenafi, Homogeneity and change point detection of hydroclimatic variables: A case study of the Ghba River Subbasin, Ethiopia, *Journal of Geography & Cartography*, 6 (2023) 1-19. <https://doi.org/10.24294/jgc.v6i1.2010>
- [10] J.C. Lehrter, Effects of land use and land cover, stream discharge, and interannual climate on the magnitude and timing of nitrogen, phosphorus, and organic carbon concentrations in three coastal plain watersheds, *Journal Water Environment Research*, 78 (2006) 2356-2368. <https://doi.org/10.2175/106143006X102015>
- [11] A.Y.M. Abdullah, A. Masrur, M.S.G. Adnan, M.A.I.A. Baky, Q.K. Hassan, Ashraf Dewan, Spatio-temporal patterns of land use/land cover change in the heterogeneous coastal region of Bangladesh between 1990 and 2017, *Journal of Remote Sensing*, 11 (2019) 790. <https://doi.org/10.3390/rs11070790>
- [12] A. Al Kafy, A. Al- Faisal, A. Al Rakib, S. Roy, J. Ferdousi, V. Raikwar, M.A. Kona, S.M. Abdullah Al Fatin, Predicting changes in land use/land cover and seasonal land surface temperature using multi-temporal landsat images in the

- northwest region of Bangladesh, *Heliyon*, 7 (2021) 07623.
<https://doi.org/10.1016/j.heliyon.2021.e07623>
- [13] M. Manfren, N. Aste, R. Moshksar, Calibration and uncertainty analysis for computer models—a meta-model based approach for integrated building energy simulation, *Journal Applied Energy*, 103 (2013) 627-641.
<https://doi.org/10.1016/j.apenergy.2012.10.031>
- [14] S. Greenland, Connecting simple and precise P-values to complex and ambiguous realities (includes rejoinder to comments on “Divergence vs. decision P-values”), *Scandinavian Journal of Statistics*, 50 (2023) 899-914.
<https://doi.org/10.1111/sjos.12645>
- [15] M. Abbott, Chapter 16 - The theory of the hydrologic model, or: the struggle for the soul of hydrology. *Advances in theoretical hydrology Elsevier*, (1992) 237-254.
<https://doi.org/10.1016/B978-0-444-89831-9.50023-5>
- [16] R.K. Price, (2011) *Urban hydroinformatics: data, models, and decision support for integrated urban water management*, IWA publishing, UK.
- [17] I.G. Pechlivanidis, B.M. Jackson, N.R. McIntyre, H.S. Wheater, Catchment scale hydrological modelling: a review of model types, calibration approaches and uncertainty analysis methods in the context of recent developments in technology and applications, *Global Nest Journal*, 13 (2011) 193-214. <https://doi.org/10.30955/gnj.000778>
- [18] H. Gao, J.L. Sabo, X. Chen, Z. Liu, Z. Yang, Z. Ren, M. Liu, Landscape heterogeneity and hydrological processes: a review of landscape-based hydrological models, *Journal Landscape ecology*, 33 (2018) 1461-1480.
<https://doi.org/10.1007/s10980-018-0690-4>
- [19] B. Li, T. Sun, F. Tian, G. Ni, Enhancing process-based hydrological models with embedded neural networks: A hybrid approach, *Journal of Hydrology*, 625 (2023) 130107.
<https://doi.org/10.1016/j.jhydrol.2023.130107>
- [20] Y. Guo, Y. Zhang, L. Zhang, Z.W. Wang, Regionalization of hydrological modeling for predicting streamflow in ungauged catchments: A comprehensive review, *John Wiley & Sons Interdisciplinary Reviews: Water*, 8 (2021) e1487.
<https://doi.org/10.1002/wat2.1487>
- [21] C. Sezen, N. Bezak, Y. Bai, M. Sraj, Hydrological modelling of karst catchment using lumped conceptual and data mining models, *Journal of Hydrology*, 576 (2019) 98-110.
<https://doi.org/10.1016/j.jhydrol.2019.06.036>
- [22] B. Getachew, B.R. Manjunatha, H.G. Bhat, Modeling projected impacts of climate and land use/land cover changes on hydrological responses in the Lake Tana Basin, upper Blue Nile River Basin, Ethiopia, *Journal of Hydrology*, 595 (2021) 125974.
<https://doi.org/10.1016/j.jhydrol.2021.125974>
- [23] P. Munoth, R. Goyal, Impacts of land use land cover change on runoff and sediment yield of Upper Tapi River Sub-Basin, India, *International Journal of River Basin Management*, 18 (2020) 177-189.
<https://doi.org/10.1080/15715124.2019.1613413>
- [24] D.F. Mekonnen, Z. Duan, T. Rientjes, M.J.H. Disse, Analysis of combined and isolated effects of land-use and land-cover changes and climate change on the upper Blue Nile River basin's streamflow, *Journal Hydrology Earth System Sciences*, 22 (2018) 6187-6207.
<https://doi.org/10.5194/hess-22-6187-2018>
- [25] M.G. Hiben, A.G. Awoke, A.A. Ashenafi, Estimation of rainfall and streamflow missing data under uncertainty for Nile basin headwaters: the case of Ghba catchments, *Journal of Applied Water Engineering & Research*, (2023) 1-15.
<https://doi.org/10.1080/23249676.2023.2230892>
- [26] M. Jajarmizadeh, S. Harun, M. Salarpour, A review on theoretical consideration and types of models in hydrology, *Journal of Environmental Science and Technology*, 5 (2012) 249-261.
- [27] G.K. Devia, B.P. Ganasri, G.S. Dwarakish, A review on hydrological models, *Journals Aquatic procedia*, 4 (2015)1001-1007.
<https://doi.org/10.1016/j.aqpro.2015.02.126>
- [28] G.E. Guzey, B. Onoz, Performance Assessment Comparison between Physically Based and Regression Hydrological Modelling: Case Study of the Euphrates–Tigris Basin, *Journal Sustainability*, 15 (2023) 10657.
<https://doi.org/10.3390/su151310657>
- [29] R.D. Pina, S. Ochoa-Rodriguez, N.E. Simoes, A. Mijic, A.S. Marques, C.J.W. Maksimovic. Semi-vs. Fully-distributed urban storm water models: model set up and comparison with two real case studies, *Water*, 8 (2016) 58.
<https://doi.org/10.3390/w8020058>
- [30] V.Y. Ivanov, E.R. Vivoni, R.L. Bras, D. Entekhabi, Catchment hydrologic response with a fully distributed triangulated irregular network model, *Water Resources Research*, 40 (2004).
<https://doi.org/10.1029/2004WR003218>
- [31] D.P. Solomatine, D.L. Shrestha, A novel method to estimate model uncertainty using machine learning techniques, *Water Resources Research*,

- 45 (2009). <https://doi.org/10.1029/2008WR006839>
- [32] T. Gebremicael, Y. Mohamed, P. Van der Zaag, Attributing the hydrological impact of different land use types and their long-term dynamics through combining parsimonious hydrological modelling, alteration analysis and PLSR analysis. *Science of the Total Environment*, 660 (2019) 1155-1167. <https://doi.org/10.1016/j.scitotenv.2019.01.085>
- [33] T. Sawunyama, (2008) Evaluating uncertainty in water resources estimation in southern Africa: A case study of South Africa, Rhodes University.
- [34] A. Ko, G. Mascaro, E.R. Vivoni, Strategies to improve and evaluate physics-based hyperresolution hydrologic simulations at regional basin scales, *Journal Water Resources Research*, 55 (2019) 1129-1152. <https://doi.org/10.1029/2018WR023521>
- [35] M. Sulis, C. Paniconi, M. Marrocu, D. Huard, D. Chaumont, Hydrologic response to multimodel climate output using a physically based model of groundwater/surface water interactions, *Water Resources Research*, 48 (2012). <https://doi.org/10.1029/2012WR012304>
- [36] DIH. MIKE HYDRO BASIN is developed by DHI, The Netherlands 2014.
- [37] [37] J.G. Arnold, R. Srinivasan, R.S. Muttiah, J.R. Williams, Large area hydrologic modeling and assessment part I: model development¹. *JAWRA Journal of the American Water Resources Association*, 34 (1998) 73-89. <https://doi.org/10.1111/j.1752-1688.1998.tb05961.x>
- [38] SEI. (1998) Water evaluation and planning system, WEAP, Stockholm Environmental Institute, Boston.
- [39] M.G. Hiben, A.G. Awoke, A.A. Ashenafi, Hydroclimatic Variability, Characterization, and Long Term Spacio-Temporal Trend Analysis of the Ghba River Subbasin, Ethiopia, *Advances in Meteorology*, (2022) 3594641. <https://doi.org/10.1155/2022/3594641>
- [40] T.G. Gebremicael, Y.A. Mohamed, P.V. Zaag, E.Y. Hagos, Temporal and spatial changes of rainfall and streamflow in the Upper Tekezē–Atbara river basin, Ethiopia, *Hydrology and Earth System Sciences*, 21 (2017) 2127-2142. <https://doi.org/10.5194/hess-21-2127-2017>
- [41] Mekelle, E. Ethiopian Institute of Technology-Mekelle, Mekelle University; 2017. Available at: https://www.researchgate.net/publication/338622745_LOCAL_CONSTRUCTION_MATERIALS_FOR_AFFORDABLE_HOUSING?
- [42] A. Zenebe, M. Vanmaercke, E. Guyassa, G. Verstraeten, J. Poesen, J. Nyssen, The Giba, Tanqwa and Tsaliel Rivers in the Headwaters of the Tekeze Basin, *Geo-trekking in Ethiopia's Tropical Mountains* Springer, (2019) 215-30. https://doi.org/10.1007/978-3-030-04955-3_14
- [43] M. Hiben, T. Goitom, T. Berhanu, Sectoral water allocation in the Ghba sub-basin. *Agricultural water management in Tigray Mekelle, Ethiopia Tigray Water Resource Bureau*, (2016) 24.
- [44] G. Aredehey, A. Mezgebu, A. Girma, The effects of land use land cover change on hydrological flow in Giba catchment, Tigray, Ethiopia, *Cogent Environmental Science*, 6(1), (2020) 1785780. <https://doi.org/10.1080/23311843.2020.1785780>
- [45] K. Wang, E.G. Davies, J. Liu, Integrated water resources management and modeling: A case study of Bow river basin, Canada, *Journal of Cleaner Production*, 240 (2019) 118242. <https://doi.org/10.1016/j.jclepro.2019.118242>
- [46] S. Naghdi, O. Bozorg-Haddad, M. Khorsandi, X. Chu, Multi-objective optimization for allocation of surface water and groundwater resources, *Science of the Total Environment*, 776 (2021) 146026. <https://doi.org/10.1016/j.scitotenv.2021.146026>
- [47] M. Ben-Daoud, B. El Mahradi, I. Elhassnaoui, A. Moumen, A. Sayad, M. ELbouhadioui, Gabriela Adina Morosanu, Lhoussaine E. Mezouary, A. Essahlaoui, S. Eljaafari, Integrated water resources management: An indicator framework for water management system assessment in the R'Dom Sub-basin, Morocco, *Environmental Challenges*, 3 (2021) 100062. <https://doi.org/10.1016/j.envc.2021.100062>
- [48] M. Beniston, M. Stoffel, Assessing the impacts of climatic change on mountain water resources, *Science of The Total Environment*, 493 (2014) 1129-1137. <https://doi.org/10.1016/j.scitotenv.2013.11.122>
- [49] Z. Hu, L. Wang, Z. Wang, Y. Hong, H. Zheng, Quantitative assessment of climate and human impacts on surface water resources in a typical semi-arid watershed in the middle reaches of the Yellow River from 1985 to 2006, *International Journal of Climatology*, 35 (2015) 97-113. <https://doi.org/10.1002/joc.3965>
- [50] A. Mehran, A. AghaKouchak, N. Nakhjiri, M.J. Stewardson, M.C. Peel, T.J. Phillips, Y. Wada, Jakin K. Ravalico, Compounding impacts of human-induced water stress and climate change on water availability, *Scientific Reports*, 7 (2017) 1-9. <https://doi.org/10.1038/s41598-017-06765-0>

- [51] A.G. Bhawe, D. Conway, S. Dessai, D.A. Stainforth, Water resource planning under future climate and socioeconomic uncertainty in the Cauvery River Basin in Karnataka, India, *Water Resources Research*, 54 (2018) 708-728. <https://doi.org/10.1002/2017WR020970>
- [52] X. Xiang, Q. Li, S. Khan, O.I. Khalaf, Urban water resource management for sustainable environment planning using artificial intelligence techniques, *Environmental Impact Assessment Review*, 86 (2021) 106515. <https://doi.org/10.1016/j.eiar.2020.106515>
- [53] X.T. Zeng, Y.P. Li, G.H. Huang, J. Liu, Modeling of water resources allocation and water quality management for supporting regional sustainability under uncertainty in an arid region, *Water Resources Management*, 31 (2017) 3699-3721. <https://doi.org/10.1007/s11269-017-1696-4>
- [54] M. Mulligan, WaterWorld: a self-parameterising, physically based model for application in data-poor but problem-rich environments globally. *Hydrology Research*, 44(5), (2013) 748-69. <https://doi.org/10.2166/nh.2012.217>
- [55] H. Liu, Y. Jia, C. Niu, H. Su, J. Wang, J. Du, M. Khaki, P. Hu, J. Liu, Development and validation of a physically-based, national-scale hydrological model in China, *Journal of Hydrology*, 590 (2020) 125431. <https://doi.org/10.1016/j.jhydrol.2020.125431>
- [56] M. Saber, T. Hamaguchi, T. Kojiri, K. Tanaka, T. Sumi, A physically based distributed hydrological model of wadi system to simulate flash floods in arid regions, *Arabian Journal of Geosciences*, 8 (2015) 143-160. <https://doi.org/10.1007/s12517-013-1190-0>
- [57] A.A. Ashenafi, (2014) Modeling hydrological responses to changes in land cover and climate in Geba River Basin, Northern Ethiopia. Freie Universität Berlin, Berlin.
- [58] Bizuneh AJFU, (2021) Modeling the Effect of Climate and Land Use Change. Available at: https://www.researchgate.net/publication/351302859_Modeling_the_effect_of_climate_and_land_use_change_on_the_water_resources_in_Northern_Ethiopia_the_case_of_Suluh_River_Basin?
- [59] T.M. Tena, P. Mwaanga, A. Nguvulu, Hydrological modelling and water resources assessment of Chongwe River Catchment using WEAP model, *Water*, 11 (2019) 839. <https://doi.org/10.3390/w11040839>
- [60] I. McNamara, A. Nauditt, M. Zambrano-Bigiarini, L. Ribbe, H. Hann, Modelling water resources for planning irrigation development in drought-prone southern Chile, *International Journal of Water Resources Development*, 37 (2021) 793-818. <https://doi.org/10.1080/07900627.2020.1768828>
- [61] I.M. Johannsen, J.C. Hengst, A. Goll, B. Hollermann, B. Diekkruger, Future of water supply and demand in the Middle Draa Valley, Morocco, under climate and land use change, *Water*, 8 (2016) 313. <https://doi.org/10.3390/w8080313>
- [62] S. Javadinejad, K. Ostad-Ali-Askari, S. Eslamian, Application of multi-index decision analysis to management scenarios considering climate change prediction in the Zayandeh Rud River Basin, *Water Conservation Science and Engineering*, 4 (2019) 53-70. <https://doi.org/10.1007/s41101-019-00068-3>
- [63] P. Kumar, R. Dasgupta, S. Dhyani, R. Kadaverugu, B.A. Johnson, S. Hashimoto, N. Sahu, R. Avtar, O. Saito, S. Chakraborty, B.K. Mishra, Scenario-Based Hydrological Modeling for Designing Climate-Resilient Coastal Water Resource Management Measures: Lessons from Brahmani River, Odisha, Eastern India, *Journal of Sustainability*, 13 (2021) 6339. <https://doi.org/10.3390/su13116339>
- [64] M. Karamouz, B. Ahmadi, Z. Zahmatkesh, Developing an agricultural planning model in a watershed considering climate change impacts, *Journal of Water Resources Planning*, 139 (2013) 349-363. [https://doi.org/10.1061/\(ASCE\)WR.1943-5452.0000263](https://doi.org/10.1061/(ASCE)WR.1943-5452.0000263)
- [65] E.H. Ellington, G. Bastille-Rousseau, C. Austin, K.N. Landolt, B.A. Pond, E.E. Rees, N. Robar, D. L. Murray, Using multiple imputation to estimate missing data in meta-regression, *Methods in Ecology & Evolution*, 6 (2015) 153-163. <https://doi.org/10.1111/2041-210X.12322>
- [66] J. Nyssen, A. Frankl, A. Zenebe, J. Deckers, J. Poesen, Development. Land management in the northern Ethiopian highlands: local and global perspectives; past, present and future, *Land Degradation Development*, 26 (2015) 759-64. <https://doi.org/10.1002/ldr.2336>
- [67] J. Nyssen, S. Tielens, T. Gebreyohannes, T. Araya, K. Teka, K. Degeyndt, K. Descheemaeker, K. Amare, M. Haile, A. Zenebe, N. Munro, K. Walraevens, K. Gebrehiwot, J. Poesen, A. Frankl, A. Tsegay, J. Deckers, Understanding spatial patterns of soils for sustainable agriculture in northern Ethiopia's tropical mountains, *Plos one*, 14 (2019) e0224041. <https://doi.org/10.1371/journal.pone.0224041>
- [68] T.G. Gebremicael, Y.A. Mohamed, E. Hagos, Temporal and spatial changes of rainfall and streamflow in the Upper Tekezē–Atbara river basin, Ethiopia, *Hydrology and Earth System*

- Sciences, 21 (2017) 2127-2142.
<https://doi.org/10.5194/hess-21-2127-2017>
- [69] J. Nyssen, S. Tielens, T. Gebreyohannes, T. Araya, K. Tekla, W. Johan Van de, K. Degeyndt, K. Descheemaeker, K. Amare, M. Haile, A. Zenebe, N. Munro, K. Walraevens, K. Gebrehiwot, J. Poesen, A. Frankl, A. Tsegay, J. Deckers, Understanding spatial patterns of soils for sustainable agriculture in northern Ethiopia's tropical mountains, PLOS ONE, 14 (2019) e0224041.
<https://doi.org/10.1371/journal.pone.0224041>
- [70] M. Behailu, N. Tadesse, A. Legesse, D. Teklu, (2004) Community based irrigation management in the Tekeze basin: Performance evaluation of small scale irrigation schemes, Mekelle University, Ethiopia.
- [71] F. Hagos, J. Pender, N. Gebreselassie, (2002) Land degradation and strategies for sustainable land management in the Ethiopian highlands. International Livestock Research Institute, 73.
- [72] S.K. Weldegebriel, K.J.S. Yeshitela, Measuring the Semi-Century Ecosystem-Service Value Variation in Mekelle City Region, Northern Ethiopia, Sustainability, 13 (2021)10015.
<https://doi.org/10.3390/su131810015>
- [73] P. Scull, J. Franklin, O.A. Chadwick, D. McArthur, Predictive soil mapping: a review. Progress in Physical geography, 27 (2003) 171-97.
<https://doi.org/10.1191/0309133303pp366ra>
- [74] W. Bedada, (2015) Compost and fertilizer-alternatives or complementary?. SLU publication database (SLU pub)
- [75] Hurni H. Soil formation rates in Ethiopia (with scale 1: 1 000 000). 1983.
- [76] N.H. Batjes ISRIC-WISE derived soil properties on a 5 by 5 arc-minutes global grid (ver. 1.2). ISRIC-World Soil Information; 2012.
- [77] D.W. Goshime, A.T. Haile, T. Rientjes, R. Absi, B. Ledésert, T. Siegfried, Implications of water abstraction on the interconnected Central Rift Valley Lakes sub-basin of Ethiopia using WEAP. Journal of Hydrology: Regional Studies, 38 (2021) 100969.
<https://doi.org/10.1016/j.ejrh.2021.100969>
- [78] A. Amin, J. Iqbal, A. Asghar, L. Ribbe, Analysis of current and future water demands in the Upper Indus Basin under IPCC climate and socio-economic scenarios using a hydro-economic WEAP model, Water, 10 (2018) 537.
<https://doi.org/10.3390/w10050537>
- [79] E. Nkiaka, N. Nawaz, J.C. Lovett, Assessment R. Effect of single and multi-site calibration techniques on hydrological model performance, parameter estimation and predictive uncertainty: a case study in the Logone catchment, Lake Chad basin, Stochastic Environmental Research, 32 (2018) 1665-1682.
<https://doi.org/10.1007/s00477-017-1466-0>
- [80] T.J.G. Sirisena, S. Maskey, R. Ranasinghe, Hydrological model calibration with streamflow and remote sensing based evapotranspiration data in a data poor basin, Remote sensing, 12 (2020) 3768. <https://doi.org/10.3390/rs12223768>
- [81] D. Espejel-Garcia, J. A. Saniger-Alba, G. Wenglas-Lara, V.V. Espejel-Garcia, A. Villalobos-Aragon, A comparison among manual and automatic calibration methods in VISSIM in an Expressway (Chihuahua, Mexico), Open Journal of Civil Engineering, 7 (2017) 539-552.
<https://doi.org/10.4236/ojce.2017.74036>
- [82] F. Pianosi, K. Beven, J. Freer, J.W. Hall, J. Rougier, D.B. Stephenson, T. Wagener, Sensitivity analysis of environmental models: A systematic review with practical workflow, Environmental Modelling & Software, 79 (2016) 214-232.
<https://doi.org/10.1016/j.envsoft.2016.02.008>
- [83] J. Gou, C. Miao, Q. Duan, Q. Tang, Z. Di, W. Liao, J. Wu, Sensitivity analysis-based automatic parameter calibration of the VIC model for streamflow simulations over China, Water Resources Research, 56 (2020) e2019WR025968.
<https://doi.org/10.1029/2019WR025968>
- [84] D. Abera Abdi, T. Ayenew, Evaluation of the WEAP model in simulating subbasin hydrology in the Central Rift Valley basin, Ethiopia, Ecological processes, 10 (2021)1-14.
<https://doi.org/10.1186/s13717-021-00305-5>
- [85] S.M. Jalilov, M. Kefi, P. Kumar, Y. Masago, B.K. Mishra, Sustainable urban water management: Application for integrated assessment in Southeast Asia, Journal of Sustainability, 10 (2018)122. <https://doi.org/10.3390/su10010122>
- [86] M.G. Hiben, G. Di Baldassarre, A. Van Griensven, Can We Model Floodplain Inundation Patterns in Data-Scarce Areas?. Ethiopian Journal of Water Science and Technology, 3 (2020) 111-129.
<https://doi.org/10.59122/135811F>
- [87] A. Ritter, R. Munoz-Carpena, Performance evaluation of hydrological models: Statistical significance for reducing subjectivity in goodness-of-fit assessments, Journal of Hydrology, 480 (2013) 33-45.
<https://doi.org/10.1016/j.jhydrol.2012.12.004>

- [88] A.W. Wood, J.C. Schaake, Correcting errors in streamflow forecast ensemble mean and spread, *Journal of Hydrometeorology*, 9 (2008) 132-148. <https://doi.org/10.1175/2007JHM862.1>
- [89] M. A. Faiz, D. Liu, Q. Fu, M. Li, F. Baig, A. A. Tahir, M.I. Khan, T. Li, S. Cui, Performance evaluation of hydrological models using ensemble of General Circulation Models in the northeastern China, *Journal of Hydrology*, 565 (2018) 599-613.
- [90] D.A. Abdi, T. Ayenew, Evaluation of the WEAP model in simulating subbasin hydrology in the Central Rift Valley basin, Ethiopia, *Ecological Processes*, 10 (2021) 1-14. <https://doi.org/10.1186/s13717-021-00305-5>
- [91] J. Craven, H. Angarita, G.A.C. Perez, D. Vasquez, Development and testing of a river basin management simulation game for integrated management of the Magdalena-Cauca river basin, *Environmental modelling software*, 90 (2017) 78-88. <https://doi.org/10.1016/j.envsoft.2017.01.002>
- [92] A. Abrishamchi, H. Alizadeh, M. Tajrishy, A. Abrishamchi, Water resources management scenario analysis in Karkheh River Basin, Iran, using WEAP model, *Hydrological Science and Technology*, 23 (2007) 1.
- [93] M. Simard, N. Pinto, J.B. Fisher, A. Baccini, Mapping forest canopy height globally with spaceborne lidar, *Journal of Geophysical Research: Biogeosciences*, 116 (2011). <https://doi.org/10.1029/2011JG001708>
- [94] D. Weindorf, Y. Zhu, Spatial variability of soil properties at Capulin volcano, New Mexico, USA: Implications for sampling strategy, *Pedosphere*, 20 (2010) 185-197. [https://doi.org/10.1016/S1002-0160\(10\)60006-9](https://doi.org/10.1016/S1002-0160(10)60006-9)
- [95] D.R. Legates, J.G. McCabe, Evaluating the use of "goodness-of-fit" measures in hydrologic and hydroclimatic model validation, *Water Resources Research*, 35 (1999) 233-241. <https://doi.org/10.1029/1998WR900018>
- [96] A. Noori, H. Bonakdari, M. Hassaninia, K. Morovati, I. Khorshidi, A. Noori, B. Gharabaghi, A reliable GIS-based FAHP-FTOPSIS model to prioritize urban water supply management scenarios: A case study in semi-arid climate, *Sustainable Cities and Society*, 81 (2022), 103846. <https://doi.org/10.1016/j.scs.2022.103846>
- [97] T. Olsson, M. Kämäräinen, D. Santos, T. Seitola, H. Tuomenvirta, R. Haavisto, W. Lavado-Casimiro, Downscaling climate projections for the Peruvian coastal Chancay-Huaral Basin to support river discharge modeling with WEAP, *Journal of Hydrology: Regional Studies*, 13 (2017) 26-42. <https://doi.org/10.1016/j.ejrh.2017.05.011>
- [98] A. Noori, H. Bonakdari, K. Morovati, B. Gharabaghi, Development of optimal water supply plan using integrated fuzzy Delphi and fuzzy ELECTRE III methods—Case study of the Gamasiab basin, *Expert Systems*, 37(5) (2020) e12568. <https://doi.org/10.1111/exsy.12568>
- [99] Q. Sun, C. Miao, Q. Duan, H. Ashouri, S. Sorooshian, K-L. Hsu, A Review of Global Precipitation Data Sets: Data Sources, Estimation, and Intercomparisons, *Reviews of Geophysics*, 56(1), (2018) 79-107. <https://doi.org/10.1002/2017RG000574>
- [100] D. Kavetski, G. Kuczera, S.W. Franks, Bayesian analysis of input uncertainty in hydrological modeling: 2. Application, *Water Resources Research*, 42(3), (2006). <https://doi.org/10.1029/2005WR004376>
- [101] MA. Gebremedhin, (2019) Spatio-temporal water resource responses to land use land cover change in semi-arid Opper Tekeze Basin, Northern Ethiopia, University of Twente The Netherlands.
- [102] E. Schmidt, B. Zemadim, (2013) Hydrological modelling of sustainable land management interventions in the Mizewa watershed of the Blue Nile basin, NBDC Technical Report.
- [103] T. Gebreyohannes, F. De Smedt, K. Walraevens, S. Gebresilassie, A. Hussien, M. Hagos, K. Amare, J. Deckers, K. Gebrehiwot, Regional groundwater flow modeling of the Geba basin, northern Ethiopia, *Hydrogeology Journal*, 25(2017) 639-655. <https://doi.org/10.1007/s10040-016-1522-8>
- [104] T. Gebreyohannes, F. De Smedt, K. Walraevens, S. Gebresilassie, A. Hussien, M. Hagos, K. Amare, J. Deckers, K. Gebrehiwot, Application of a spatially distributed water balance model for assessing surface water and groundwater resources in the Geba basin, Tigray, Ethiopia, *Journal of Hydrology*, 499 (2013) 110-123. <https://doi.org/10.1016/j.jhydrol.2013.06.026>

Acknowledgment

MG Water Resource Consultancy Firm provided funding for the research project reported in this publication. The Ministry of Water and Energy (Ethiopia) provided water resource data, while the Ethiopian National Meteorological Services Agency provided climate data. The authors are very appreciative of both of these sources.

Author contributions

Conceptualization, MGH and AGA; methodology, MGH; software, MGH; validation, MGH, AGA and AAA; formal analysis, MGH; investigation, AGA; resources, AAA; data curation, MGH; writing original draft preparation, MGH; writing review & editing, AAA; visualization, AAA; supervision, AGA; project administration, AGA; funding acquisition, MGH.

Has this article screened for similarity?

Yes

Conflict of Interest

The Authors have no conflicts of interest on this article to declare.

About the License

© The Author(s) 2023. The text of this article is open access and licensed under a Creative Commons Attribution 4.0 International License.